

GE, B., HU, L., YU, X., WANG, L., FERNANDEZ, C., YANG, N., LIANG, Q. and YANG, Q.-H. 2024. Engineering triple-phase interfaces around the anode toward practical alkali metal-air batteries. *Advanced materials* [online], 36(27), article number 2400937. Available from: <https://doi.org/10.1002/adma.202400937>

# Engineering triple-phase interfaces around the anode toward practical alkali metal-air batteries.

GE, B., HU, L., YU, X., WANG, L., FERNANDEZ, C., YANG, N., LIANG, Q.  
and YANG, Q.-H.

2024

*This is the peer reviewed version of the following article: GE, B., HU, L., YU, X., WANG, L., FERNANDEZ, C., YANG, N., LIANG, Q. and YANG, Q.-H. 2024. Engineering triple-phase interfaces around the anode toward practical alkali metal-air batteries. Advanced materials [online], 36(27), article number 2400937, which has been published in final form at <https://doi.org/10.1002/adma.202400937>. This article may be used for non-commercial purposes in accordance with Wiley Terms and Conditions for Use of Self-Archived Versions. This article may not be enhanced, enriched or otherwise transformed into a derivative work, without express permission from Wiley or by statutory rights under applicable legislation. Copyright notices must not be removed, obscured or modified. The article must be linked to Wiley's version of record on Wiley Online Library and any embedding, framing or otherwise making available the article or pages thereof by third parties from platforms, services and websites other than Wiley Online Library must be prohibited.*

# Engineering Triple-Phase Interfaces around the Anode toward Practical Alkali Metal-Air Batteries

Bingcheng Ge<sup>1</sup>, Liang Hu<sup>1</sup>, Xiaoliang Yu<sup>1\*</sup>, Lixu Wang<sup>2</sup>, Carlos Fernandez<sup>3</sup>, Nianjun Yang<sup>4</sup>, Qinghua Liang<sup>5,\*</sup> and Quan-Hong Yang<sup>6\*</sup>

<sup>1</sup> Department of Mechanical Engineering and Research Institute for Smart Energy, The Hong Kong Polytechnic University Hong Kong 999077, China

<sup>2</sup> Fujian XFH New Energy Materials Co, Ltd No. 38, Shuidong Industry Park, Yongan 366000, China

<sup>3</sup> School of Pharmacy and Life Sciences Robert Gordon University Aberdeen AB107QB, UK

<sup>4</sup> Department of Chemistry & IMO-IMOMEC Hasselt University Diepenbeek 3590, Belgium

<sup>5</sup> Key Laboratory of Rare Earth Ganjiang Innovation Academy Chinese Academy of Sciences Ganzhou, Jiangxi 341000, China

<sup>6</sup> Nanoyang Group Tianjin Key Laboratory of Advanced Carbon and Electrochemical Energy Storage School of Chemical Engineering and Technology, Tianjin University, Tianjin 300072, China

## Abstract

Alkali metal-air batteries (AMABs) promise ultrahigh gravimetric energy densities, while the inherent poor cycle stability hinders their practical application. To address this challenge, most previous efforts are devoted to advancing the air cathodes with high electrocatalytic activity. Recent studies have underlined the solid-liquid-gas triple-phase interface around the anode can play far more significant roles than previously acknowledged by the scientific community. Besides the bottlenecks of uncontrollable dendrite growth and gas evolution in conventional alkali metal batteries, the corrosive gases, intermediate oxygen species, and redox mediators in AMABs cause more severe anode corrosion and structural collapse, posing greater challenges to the stabilization of the anode triple-phase interface. This work aims to provide a timely perspective on the anode interface engineering for durable AMABs. Taking the Li-air battery as a typical example, this critical review shows the latest developed anode stabilization strategies, including formulating electrolytes to build protective interphases, fabricating advanced anodes to improve their anti-corrosion capability, and designing functional separator to shield the corrosive species. Finally, the remaining scientific and technical issues from the prospects of anode interface engineering are highlighted, particularly materials system engineering, for the practical use of AMABs.

## Keywords

alkali metal-air batteries, anode engineering, electrolyte formulation, functional separator, triple-phase interfaces

## 1. Introduction

Rechargeable lithium-ion batteries (LIBs) have dominated the global energy storage market, including portable electronics, electrified transportation, and large-scale grid storage.<sup>[1-3]</sup> Since their first successful commercialization, the theoretical energy density limit based on Li-intercalation chemistry has been approached after 30 years of development.<sup>[4]</sup> The growing demand to further increase energy density has accelerated the investigation of new energy storage technologies beyond Li-ion batteries.<sup>[5-7]</sup> Non-aqueous alkali metal-air batteries (AMABs) have emerged as one of the most promising alternatives to traditional LIBs for next-generation energy storage. Unlike LIBs utilizing intercalation compounds of heavy equivalent weight as electrode materials, an AMAB typically comprises an alkali metal anode and a porous air cathode.<sup>[8-12]</sup> For instance, Li-air battery (LAB) delivers an ultrahigh potential energy density of  $\approx 11\,400\text{ Wh kg}^{-1}$  based on the reaction of  $2\text{Li} + \text{O}_2 \leftrightarrow \text{Li}_2\text{O}_2$  ( $E^0 = 2.96\text{ V vs Li}^+/\text{Li}$ ), which is comparable to that of gasoline ( $13\,000\text{ Wh kg}^{-1}$ ) (Figure 1a).<sup>[13-16]</sup> In AMABs, the metal anode and air cathode are separated by a separator soaked with electrolytes.<sup>[6,17-19]</sup> The electrochemical reactions at two electrodes are shown below:-

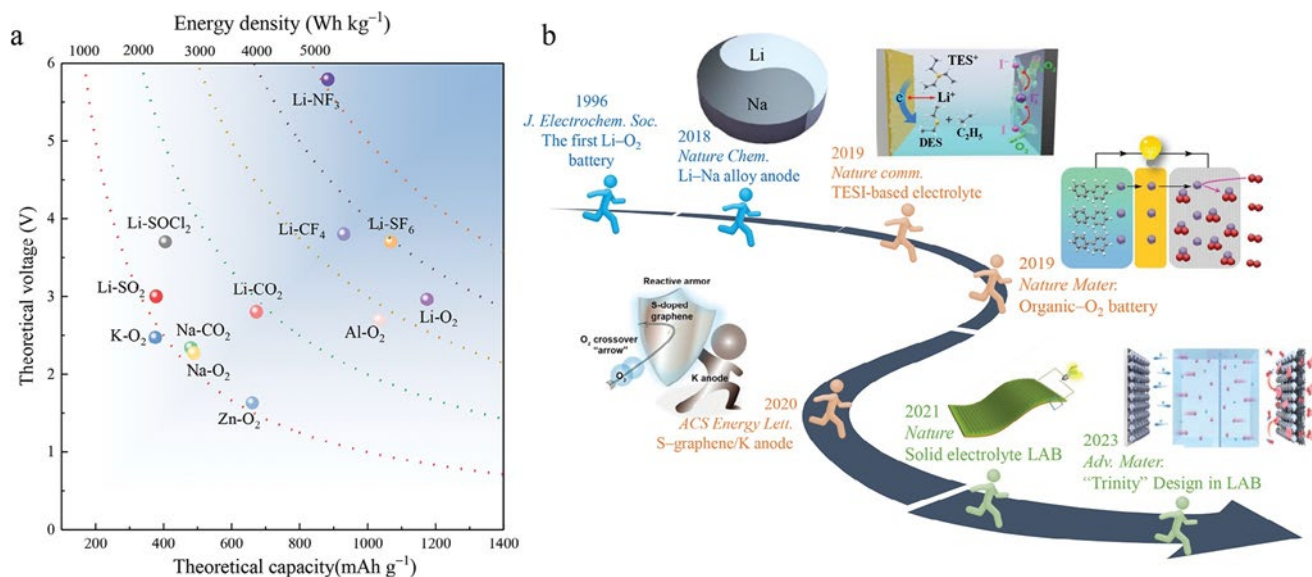
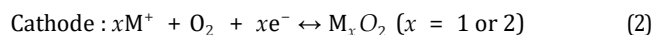


**Figure 1.** Advanced AMABs for next-generation high-density energy storage. a) Energy density comparison among various high-energy battery technologies.<sup>[61–72]</sup> b) The main progress in the anode stabilization of AMABs (Li-Na alloy anode). Reproduced with permission.<sup>[53]</sup> Copyright 2018, Springer Nature. TESI-based electrolyte. Reproduced with permission.<sup>[73]</sup> Copyright 2019, Springer Nature. Organic-O<sub>2</sub> battery. Reproduced with permission.<sup>[74]</sup> Copyright 2019, Springer Nature. S-graphene/K anode. Reproduced with permission.<sup>[75]</sup> Copyright 2020, American Chemical Society. Solid electrolyte LAB. Reproduced with permission.<sup>[76]</sup> Copyright 2021, Springer Nature. "Trinity" design in LAB. Reproduced with permission.<sup>[77]</sup> Copyright 2023, Wiley-VCH GmbH.

In the initial discharge process, alkali metal (M) is oxidized to M<sup>+</sup> at the anode side. At the same time, multi-step reduction of O<sub>2</sub> occurs at the cathode side, first to thermodynamically unstable superoxide (O<sub>2</sub><sup>-</sup>) and then to more stable peroxide (O<sub>2</sub><sup>2-</sup>).<sup>[20,21]</sup> The as-generated O<sub>2</sub><sup>2-</sup> combines with M<sup>+</sup> to form insoluble M<sub>x</sub>O<sub>2</sub> deposits.<sup>[22,23]</sup> Upon charging, M<sub>x</sub>O<sub>2</sub> are expected to be reversely oxidized to release O<sub>2</sub> and M<sup>+</sup>. The charge transfer processes are mediated by the reactive oxygen, including O<sub>2</sub><sup>-</sup>, O<sub>2</sub><sup>2-</sup>, and singlet oxygen (<sup>1</sup>O<sub>2</sub>),<sup>[24]</sup> which unfortunately tend to decelerate the reaction kinetics.<sup>[25]</sup> Moreover, these oxygen species are corrosive, which may continuously degrade the electrolyte and metal anode, causing unsatisfactory cycling durability and poor round-trip efficiency of AMABs.<sup>[26–28]</sup>

To address the above issues, a significant amount of studies have been conducted to boost the reversibility and kinetics of oxygen reduction at the air cathode in the past decades.<sup>[29–32]</sup> A broad and in-depth understanding of the cathode chemistry in AMABs has been built, and (electro)chemically stable and high-surface-area air cathodes with excellent electrocatalytic activities toward oxygen reduction/oxidation have been developed.<sup>[29,33–37]</sup> The 3D structure of the cathode has been proved to be conducive to the improvement of the catalytic activity of the cathode. For example, Seokwoo Jeon et al. investigated the effects of homogenized triple-phase boundaries on the reaction kinetics in air cathodes, they found that compared with the random porous Cu foam, the favorable structural design of 3D Cu can effectively improve the energy efficiency.<sup>[38]</sup> However, many recent studies revealed that the poor interfacial stability of the alkali metal anode is another bottleneck restricting the practical applications of AMABs.<sup>[39,40]</sup> In particular, the open environment containing mixing gas species of O<sub>2</sub>, CO<sub>2</sub>, and H<sub>2</sub>O in the AMAB electrolyte results in complex electrochemical reactions.<sup>[41]</sup> The alkali metal anode is confronted with a complex solid (metal anode)–liquid (the electrolyte)–gas (ambient air) triple-phase interface.<sup>[42]</sup> The crossover of O<sub>2</sub>/CO<sub>2</sub>/N<sub>2</sub>, trace H<sub>2</sub>O, and redox mediators (RMs) from the cathode to the anode causes severe parasitic reactions with the metal anode and, thus performance deterioration of AMABs.<sup>[43–45]</sup> The reactive oxygen intermediates like the highly nucleophilic O<sub>2</sub><sup>-</sup>, O<sub>2</sub><sup>2-</sup>, and <sup>1</sup>O<sub>2</sub> may interfere with the O<sub>2</sub> electrochemistry.<sup>[46,47]</sup> Besides, the uncontrollable dendrite growth derived from uneven metal deposition and inhomogeneous SEI deteriorates at the complex triple-phase anodic interface and easier structural collapse of anodes.<sup>[48,49]</sup> Hence, enhancing the stability of the triple-phase interface around the anode is pivotal for the development of AMABs for practical applications.

Stabilizing the anode interface of AMABs is thus quite challenging. In recent years, numerous strategies have been developed to address these challenges,<sup>[19,50,51]</sup> such as the utilization of alternative anode chemistry with lower reactivity,<sup>[52,53]</sup> novel electrolyte formulation for building protective interphases and reducing corrosive attacks,<sup>[54-56]</sup> and fabrication of ion-selective membranes/scaffolds to shield the corrosive species.<sup>[57-60]</sup> Unfortunately, still no review or perspective covers recent advancements in this promising research direction. To fill this void, recent progress on stabilizing the anode interfaces is reviewed comprehensively in this work to provide easy and timely access for readers to follow the latest developments in the anodic interface area. In this critical review, we first overview the alkali metal anode electrochemistry for AMABs and the current challenges by examining lithium-air batteries (LABs) as a typical example. We then discuss the recent progress in stabilizing the solid-liquid-gas interface of alkali metal anodes by various strategies, such as electrolyte formulation, advanced metal anode construction, and separator modification (Figure 1b). We also highlight recent advances in constructing high-performance Na/K-air batteries. Finally, we shed light on the current limitations and the future scopes for stabilizing anode interfaces, aiming to inspire the construction of stable anodic interfaces for next-generation AMABs.

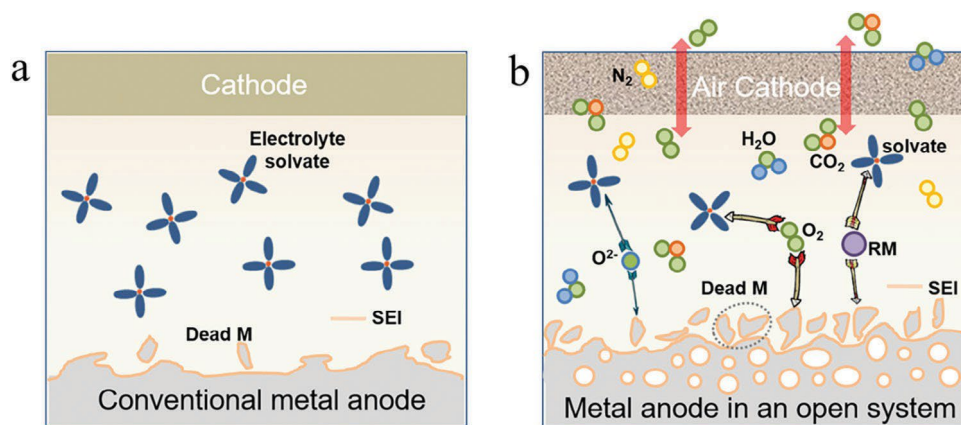


**Figure 2.** Challenges for the stabilization of triple-phase interfaces around the anodes in AMABs. The comparison between two-phase and triple-phase interfacial reactions of metal anodes in conventional a) alkali metal batteries and b) AMABs.

## 2. Challenges for Stabilizing the Triple-Phase Interfaces around the Anodes in AMABs

Compared to the two-phase interface at the anode in conventional alkali metal batteries, the complex triple-phase reactions at the anode interface cause more uncontrollable growth of “dead” alkali metal and dendrites, easier cracking and continuous generation of passivating SEI, and more severe structural collapse of the metal anode (Figure 2). Among various AMAB technologies, LABs have been the most widely studied. Therefore, the following discussion focuses on the challenges toward stabilized anode interfaces in LABs, including electrolyte degradation, cross-contamination of atmospheric gases, corrosion of alkali metal anodes by reactive species, and structural collapse of metal anodes.

### 2.1. Deterioration of Electrolytes

Aprotic electrolytes between the cathode and anode have been widely used to mediate the  $\text{Li}^+$ -ion transfer in LABs.<sup>[78]</sup> The electrochemical performances of LABs are highly dependent on the properties of electrolytes, especially their stability against the nucleophilic attack by reactive oxygen species, such as  $\text{O}_2^-$ ,  $\text{O}_2^{2-}$ , and  $^1\text{O}_2$ .<sup>[26,79]</sup> These nucleophilic reactions could accelerate the decomposition of electrolytes.<sup>[80]</sup> For instance, carbonate-based electrolytes used in early LAB studies were found to decompose severely owing to the nucleophilic attacks by  $\text{O}_2^-$  on the  $\text{C}=\text{O}$  groups, producing Li alkyl carbonates and  $\text{Li}_2\text{CO}_3$ .<sup>[28]</sup> Yang and co-workers revealed that auto-oxidation via  $\alpha$ -H abstraction occurs when mixing ether solvents with  $\text{O}_2$ .<sup>[81]</sup> It promotes the release of protons, esterification, and then polymerization, thus degrading the electrolyte.

Moreover, the LAB system is exposed to atmospheric moisture. The polar water molecules interact with the carbonyl groups with high electronegativity and metastable double bonds in the electrolyte components, giving rise to complex side products.<sup>[82]</sup> Therefore, hydrophobic electrolytes with low water solubility are more favorable. To date, it is still a crucial challenge to formulate proper electrolytes in AMABs with low volatility, high hydrophobicity, and good resistance to the attack of oxygen groups.

## 2.2. Cross-Contamination of Atmospheric Gases

Another main challenge for stabilizing anodic interfaces in AM-ABs is the cross-contamination of atmospheric O<sub>2</sub>, CO<sub>2</sub>, N<sub>2</sub>, and H<sub>2</sub>O gases.<sup>[44,83,84]</sup> An open atmosphere is more likely designed to supply continuous O<sub>2</sub> at the cathode of AMABs. However, the simultaneous exposure of electrolytes and Li anodes to the air leads to corrosion and thus the formation of Li-ion insulating salts like Li<sub>2</sub>O, Li<sub>2</sub>CO<sub>3</sub>, and LiOH at the anodic interfaces.

The crossover of oxygen was first documented by Assary et al.<sup>[41]</sup> Their observations revealed the presence of multiple oxidative products at the anode, including LiOH, Li<sub>2</sub>CO<sub>3</sub>, CH<sub>3</sub>Oli, CH<sub>3</sub>Li, and polymeric layers. Also, the shuttled oxygen from the cathode reacts with the fresh Li metal and dendrites at the anode, resulting in the passivation of the anodic interface. It brings about severe polarization, shortened cycle life, and even safety concerns. Therefore, protecting the Li anode against O<sub>2</sub> is crucial for the safe and durable operation of LABs.

As mentioned above, H<sub>2</sub>O is another critical corrosive gas component in ambient air, which reacts with Li to form LiOH and H<sub>2</sub> through the following equation:<sup>[44]</sup>



Similar to the above oxygen-containing species, the presence of H<sub>2</sub>O also leads to the corrosion of Li metal. Water pollution induces solution-mediated parasitic chemical and electrochemical reactions to produce porous LiOH and LiOOH, which may destroy the SEI structure and aggravate the corrosion of the anode.<sup>[44,85,86]</sup> The continuous depletion of cell components due to the irreversible transformation of the lithium anode results in a deterioration of battery cyclability.

The research community has also confirmed that the CO<sub>2</sub>/N<sub>2</sub> gases degrade the electrochemical performance of LABs.<sup>[43,83]</sup> These gases were revealed to participate in the discharge process in a complex way, forming irreversible Li<sub>2</sub>CO<sub>3</sub> and Li<sub>3</sub>N products.<sup>[87,88]</sup> A higher energy barrier exists for decomposing Li<sub>2</sub>CO<sub>3</sub>/Li<sub>3</sub>N than Li<sub>2</sub>O<sub>2</sub>, resulting in high charge overpotentials, low Coulombic efficiencies, and short battery lifespan.<sup>[89]</sup> For example, CO<sub>2</sub> reacts with Li through the following equation:



Although it has been reported that protective Li<sub>2</sub>CO<sub>3</sub> film can be formed after immersing the Li anode in the CO<sub>2</sub> atmosphere,<sup>[90]</sup> the practical reactions involved in ambient air could be much more complex. Thus, the Li<sub>2</sub>CO<sub>3</sub> product is probably not integrated into the as-generated SEI in a well-organized way. As such, it may reduce the efficiency and reversibility of the anodic reaction, increasing overpotential at the Li anode.<sup>[91,92]</sup>

## 2.3. Corrosion of Metal Anodes by Reactive Species in Electrolytes

The corrosive species such as O<sub>2</sub><sup>2-</sup>, O<sub>2</sub><sup>-</sup>, and <sup>1</sup>O<sub>2</sub> generated during the discharge process are highly nucleophilic radicals that could cause continuous anode corrosion. Various byproducts of Li<sub>2</sub>O, Li<sub>2</sub>O<sub>2</sub>, Li<sub>2</sub>CO<sub>3</sub>, and insoluble ionic Li compounds would be produced.<sup>[41,93]</sup> Moreover, the high reactivity of the metal anode not only causes parasitic reactions with oxygen groups in the electrolyte and the introduced redox mediators (RMs).<sup>[45]</sup> Generally, the RMs serve as mobile charge carriers in the local areas of the air cathode.<sup>[19]</sup> They are oxidized upon charging to produce RM<sup>+</sup> and react with Li<sub>2</sub>O<sub>2</sub>.<sup>[45]</sup> However, RM<sup>+</sup> in the electrolyte could also diffuse through the electrolyte and separator to corrode the Li anode, generating the well-known redox shuttling effect.<sup>[94]</sup>

## 2.4. Structure Collapse of the Alkali Metal Anodes

The degeneration of the Li metal anode mainly originates from its high activity and hostless nature. The direct contact between the alkali metal anode and O<sub>2</sub> leads to redox reactions that produce reduced oxygen species, such as superoxides.<sup>[41,95]</sup> Under ideal conditions, the final product of Li<sub>2</sub>O helps to build a protective SEI layer to prevent further reactions between Li and O<sub>2</sub>.<sup>[96]</sup> However, at the complex solid-liquid-gas triple-phase interface, breakage of the practical SEI layers easily occurs because of the severe volume fluctuation and erosion by corrosive species, exposing fresh Li metal to the electrolyte. Thus, continuous parasitic reactions happen at the anodic interface during repeated charge-discharge cycles, eventually leading to the structure collapses of Li anodes.<sup>[97]</sup>

## 3. Electrolyte Engineering

The electrolyte is a critical component mediating the transfer of ionic charge carriers between the cathode and anode in an LAB. It plays a vital role in determining the solubility of oxygen, the formation pathway of Li<sub>2</sub>O<sub>2</sub>, and the production of the SEI layer at the anodic interface.<sup>[26]</sup> Indeed, corrosion of Li anodes has been extensively observed in conventional electrolytes over prolonged charge-

discharge cycles.<sup>[97]</sup> A careful selection of electrolytes is necessary for the durable operation of LABs in the open atmosphere, given the hyper-reactivity of the metallic anode and dendrite growth-derived safety concerns. Based on numerous studies over the past decades, ideal electrolytes in LABs should have the following merits: 1) good compatibility with the metal anode to produce stable SEI; 2) low volatility, poor wetting ability, and nonflammability to be compatible with the open system; 3) high chemical and electrochemical stability toward oxygen, and the reduced oxygen species of  $O_2^-$ ,  $O_2^{2-}$ , and  $^1O_2$ ; 4) a wide voltage window for efficient battery operation.<sup>[98-100]</sup> **Table 1** summarizes some recent advances based on electrolyte alternatives to improve the performance of Li-air batteries. In this section, research progress on designing functional liquid electrolytes and solid-state electrolytes toward stabilized anodic interfaces will be thoroughly reviewed.

### 3.1. Novel Liquid Electrolytes for Stabilizing the Anode Interfaces

Liquid electrolytes are preferred in battery systems because of their easy formulation, low viscosity, large ionic conductivity, and good electrode wettability. They are generally composed of high-purity single or mixed solvents and alkali metal salts. Generally, the stability of liquid electrolytes against metal anodes and corrosive gases/species depends on the choice of electrolyte components, especially the introduced functional additives. In the following section, various functional additives in liquid electrolytes for stabilizing anodic interfaces will be highlighted, focusing on their different functions, including constructing protective SEI, inhibiting cross-gas contamination, and alleviating attacks by corrosive species.<sup>[113-115]</sup>

**Table 1.** Electrochemical performances of Li-air batteries with different electrolytes and operation parameters.

Electrolyte	Cycles	Capacity	Current density	Operating environment	Ref
0.5 m LiTFSI in G2 with 5 mm PDI-TEMPO	450	0.25 mAh cm <sup>-2</sup>	0.2 mA cm <sup>-2</sup>	O <sub>2</sub>	[47]
1 m LiTFSI in G4 with C <sub>2</sub> H <sub>5</sub> N <sub>3</sub> S <sub>2</sub>	90	0.5 mAh cm <sup>-2</sup>	0.1 mA g <sup>-1</sup>	O <sub>2</sub>	[55]
0.5 m Mlithiated Nafion in DMSO	225	1000 mAh g <sup>-1</sup>	500 mA g <sup>-1</sup>	O <sub>2</sub>	[56]
1.0 m LiTFSI/G4 electrolyte with 50 mm TESI	60	1000 mAh g <sup>-1</sup>	500 mA g <sup>-1</sup>	O <sub>2</sub>	[73]
Lithium-ion-exchanged zeolite X	150	1000 mAh g <sup>-1</sup>	500 mA g <sup>-1</sup>	Air	[76]
0.1 m LiClO <sub>4</sub> in HMPA	100	1000 mAh g <sup>-1</sup>	200 mA g <sup>-1</sup>	O <sub>2</sub>	[101]
1m LiClO <sub>4</sub> / DMSO with MNOFs	50	1000 mAh g <sup>-1</sup>	0.1 mA g <sup>-1</sup>	O <sub>2</sub>	[102]
1 m LiTFSI/G4 with 200 mm RhB	215	1000 mAh g <sup>-1</sup>	500 mA g <sup>-1</sup>	O <sub>2</sub>	[103]
50 mm tetrathiafulvalene with 50 mm LiCl /G2	100	1000 mAh g <sup>-1</sup>	200 mA g <sup>-1</sup>	O <sub>2</sub>	[104]
1 m LiSO <sub>3</sub> CF <sub>3</sub> in G4	120	1000 mAh g <sup>-1</sup>	300 mA g <sup>-1</sup>	O <sub>2</sub>	[105]
2,2,2-trichloroethyl LiTFSI in G4 with 10-methylphenothiazine	50	1000 mAh g <sup>-1</sup>	1000 mA g <sup>-1</sup>	O <sub>2</sub>	[106]
1 m LiCF <sub>3</sub> SO <sub>3</sub> in G4 with 5 wt% TEOS	144	1000 mAh g <sup>-1</sup>	300 mA g <sup>-1</sup>	O <sub>2</sub>	[107]
1.0 m LiTFSI/G4 with 50 mm redox mediators	150	500 mAh g <sup>-1</sup>	200 mA g <sup>-1</sup>	O <sub>2</sub>	[108]
5.0 m LiNO <sub>3</sub> in DMA with 2,2,6,6-tetramethyl-1-piperidinyloxy	100	500 mA g <sup>-1</sup>	200 mA g <sup>-1</sup>	O <sub>2</sub>	[109]
1 m LiTFSI/G4 with 100 mm Lil and 100 mm DMPH	438	500 mAh g <sup>-1</sup>	200 mA g <sup>-1</sup>	O <sub>2</sub>	[110]
1m LiClO <sub>4</sub> in DMSO with 50 mm IMPBr	50	500 mAh g <sup>-1</sup>	800 mA g <sup>-1</sup>	O <sub>2</sub>	[111]
Li <sub>1.35</sub> T <sub>1.75</sub> Al <sub>0.25</sub> P <sub>2.7</sub> Si <sub>0.3</sub> O <sub>12</sub>	100	2000 mAh g <sup>-1</sup>	200 mA g <sup>-1</sup>	Air	[112]

Wesley et al. demonstrated for the first time the durable cycling of Li anode in a straight-chain alkyl amide-based electrolyte when lithium nitrate (LiNO<sub>3</sub>) was introduced, which effectively stabilized the SEI of Li anode and inhibited the reaction between the solvent and Li anode.<sup>[116]</sup> Similarly, Roberts et al. used LiNO<sub>3</sub> as an effective additive to stabilize the dimethyl sulfoxide (DMSO) solvent incompatible with metallic Li.<sup>[117]</sup> An efficient passivation film was formed, which was revealed to be self-healing and could facilitate long-term cycling once damaged. Subsequently, Kubo et al. introduced both LiBr and LiNO<sub>3</sub> in a tetramethylene glycol dimethyl ether (TEGDME)-based LAB electrolyte.<sup>[113]</sup> The NO<sub>3</sub><sup>-</sup> anion oxidizes the Li anode surface to inhibit the shuttle reaction, while the Br<sup>-</sup>/Br<sub>3</sub><sup>-</sup> couple serves as an RM to facilitate oxidation at the cathode. It was also found that the mixed Br<sup>-</sup>/NO<sub>3</sub><sup>-</sup> anions act synergically to significantly suppress the parasitic reaction and dendrite formation by forming a thin and solid Li<sub>2</sub>O film (≈10 nm) on the Li anode surface.

Sun et al. reported the introduction of  $\text{InBr}_3$  as a self-defense RM in the LAB electrolyte.<sup>[118]</sup> An In-enriched composite protective layer is formed in situ on the Li anode due to the existence of  $\text{In}^{3+}$ , which effectively suppresses the side reaction between the Li anode and the electrolyte, thus improving the anodic interfacial stability. Zhang et al. reported that tetraethyl orthosilicate (TEOS) as an electrolyte additive could react with the generated LiOH at the Li surface to form a self-healing protective film (**Figure 3a**).<sup>[107]</sup> Even after the prolonged cycling in the highly corrosive system, the destructed film can be dynamically repaired via a continuous reaction between TEOS and LiOH (**Figure 3b**). Therefore, the reversibility and cycle stability of Li anodes is significantly improved (**Figure 3c,d**).

Recall that the cross-gas contamination of atmospheric  $\text{O}_2$ ,  $\text{CO}_2$ ,  $\text{N}_2$ , and  $\text{H}_2\text{O}$  gases is the main challenge for stabilizing anodic interfaces in LABs. Except for constructing a protective SEI at the Li anode surface, reducing the solubility of atmospheric gases and decelerating their diffusivities in the electrolyte is another efficient approach to address this issue. For example, Zhang et al. introduced a 10 wt% hydrophobic silica colloid electrolyte (HSCE) to protect the Li metal anode from severe corrosion and irregular dendrite growth in the Li- $\text{O}_2$  battery.<sup>[119]</sup> The results demonstrate that a lower diffusion coefficient can yield an anti-corrosion effect 980 times more effective than 0 wt% HSCE (**Figure 4a**). The in situ coupling of  $\text{CF}_3\text{SO}_3^-$  on silica surfaces via electrostatic interactions avoids the formation of a strong electrical field caused by anion depletion. It induces the production of a stable SEI and constrains the repeated SEI formation/breakage process. Moreover, the severe corrosion by  $\text{O}_2$ ,  $\text{H}_2\text{O}$ , and other contaminants can be effectively alleviated (**Figure 4b**). Consequently, a stable plating/stripping process is achieved with a long anodic lifespan of 550 cycles in Li- $\text{O}_2$  batteries.

The introduced RMs and in situ generated oxygen-containing groups over charge-discharge cycles are corrosive species in the electrolyte. They may accelerate the electrolyte decomposition and unstable SEI formation, thus continuously corroding the metal anode interfaces.<sup>[115,120,121]</sup> As a typical example, the soluble superoxide anion  $\text{O}_2^-$  coming from  $\text{LiO}_2$  may cause drastic deterioration of the electrolyte in LABs.<sup>[122]</sup> To inhibit the attack by corrosive  $\text{O}_2^-$  and  $^1\text{O}_2$ , Wang et al. designed and synthesized a multifunctional diimide-based quencher (PDI-TEMPO) for boosting the performance of LABs (**Figure 4c**).<sup>[47]</sup> The PDI-TEMPO molecule contains a PDI backbone capable of quenching  $\text{O}_2^{*-}$  and redox mediator-active TEMPO moieties to catalyze discharge and charge processes. As a result, corrosion of the metal anode is effectively inhibited, which would lead to a long cycle life (**Figure 4d,e**).

Chen et al. reported using the imidazolium cation bromide (1-methyl, 3-phenyl, 1H imidazolium bromide, IMPBr) as a tri-functional additive for LABs.<sup>[111]</sup> It enhances the redox reaction activity at the cathode side and enables dendrite-free Li deposition. The positively charged  $\text{IMP}^+$  was absorbed on the Li anode surface by electric attraction and participated in the construction of a stable SEI film, thereby protecting the Li anode from the corrosion of DMSO,  $\text{Br}^{3-}$ , and  $\text{Br}_2$ . Zhang et al. proposed to use a highly concentrated electrolyte based on LiTFSI in DMSO,<sup>[123]</sup> which has a higher Gibbs activation energy barrier for C-H bond scission from  $\text{CH}_3$  in DMSO solvent, therefore improving the electrolyte stability against  $\text{O}_2^{*-}$  attack.

To summarize, this section reviews recent important progress in developing novel liquid electrolytes for stabilized anodic interfaces in LABs.<sup>[118,124,125]</sup> While most reports focused on introducing functional additives for fabricating stable SEI against deterioration, interesting attempts have also been proposed to decelerate the diffusion of corrosive species in electrolytes. Also, super-concentrated electrolytes can alter the solvation structure and enhance the anti-corrosive capability against corrosive species.<sup>[123,126]</sup> Despite the great progress, the anodic reversibility and cycle life are still unsatisfactory. Potential safety risks exist because of easy leakage of liquid electrolytes in the open system and Li dendrite-induced short circuit issues.<sup>[57,127]</sup>

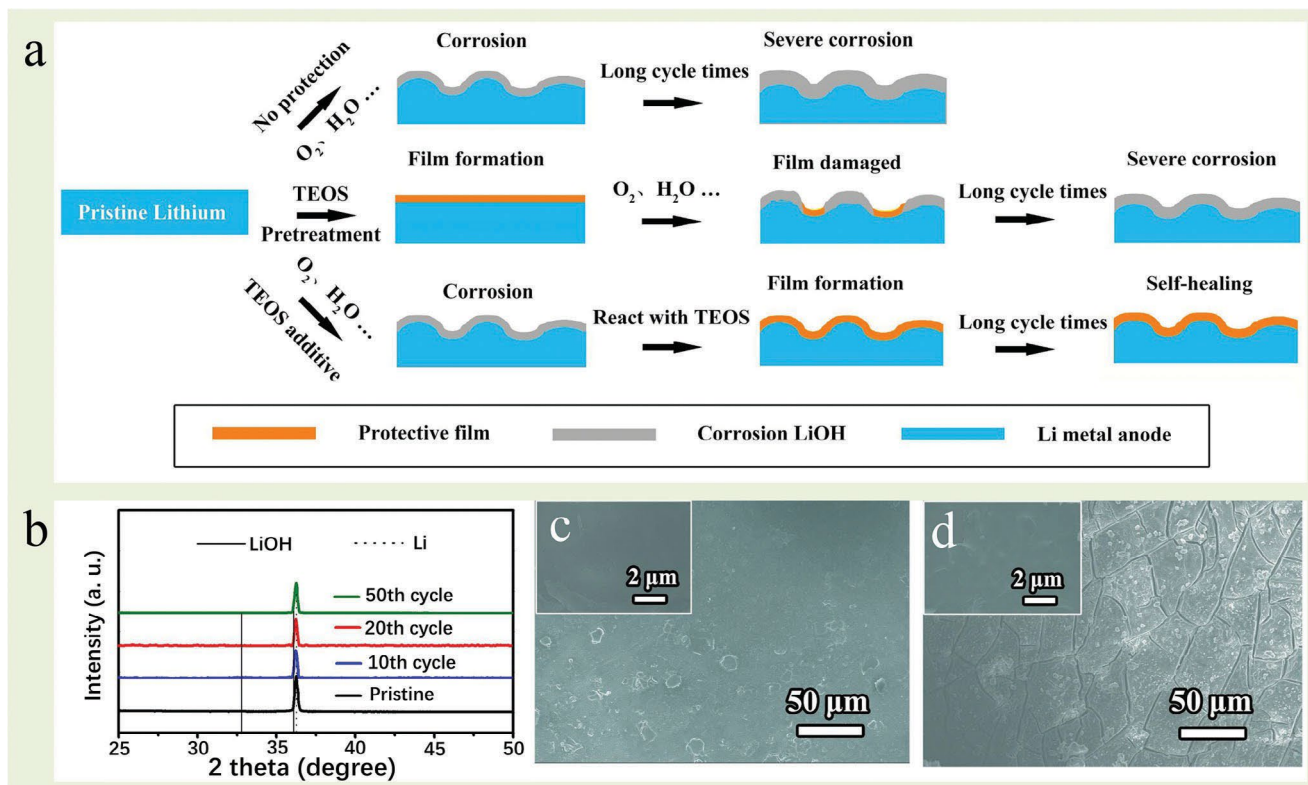


**Figure 3.** Liquid electrolyte additive-induced protective SEI for stabilizing the anode interfaces of LABs. a) A comparative analysis of the protection mechanisms for three types of Li anodes. b–d) XRD patterns and SEM images (pristine and 20th cycles) taken from TAL anodes. Reproduced with permission.<sup>[107]</sup> Copyright 2019, Elsevier.

### 3.2. Solid-State Electrolyte Engineering

Using solid-state electrolytes (SSEs) to replace liquid electrolytes has been regarded as a practical approach to address the above electrolyte leakage and dendrite-derived safety concerns.<sup>[128]</sup> SSEs comprise ceramics and/or polymeric materials to convey Li ions between the air cathode and the lithium metal anode.<sup>[129]</sup> The use of SSEs in LABs is favorable for solving the (electro)chemical problems associated with liquid organic electrolytes like instability, flammability, toxicity, and volatility.<sup>[112]</sup> The migration of reactive oxygen reduction products from the cathode to the anode can be prevented, and Li dendrite growth can also be inhibited because of their high mechanical strength.<sup>[130,131]</sup> In the following section, the progress in the development of solid polymer electrolytes (SPEs) and ceramic solid electrolytes (CSEs) in LABs will be comprehensively reviewed.

SPEs have relatively higher stability than non-aqueous liquid electrolytes in LABs. It protects the Li anode from directly reacting with  $O_2$  or  $H_2O$ . Nan et al. designed a freestanding, Li-ion conductive ultra-dry polymer electrolyte (UDPE) without additional liquid electrolyte (Figure 5a,b).<sup>[132]</sup> UDPEs can effectively inhibit the crossover of  $O_2$  to the Li metal anode (Figure 5c–h). Therefore, most unwanted side reactions between the liquid plasticizers and the highly active oxygen species were avoided in as-fabricated LABs. As such, the accumulation of  $Li_2CO_3$ / $LiOH$  by-products was also eliminated. As a result, the cycle life of UDPE-based LABs was twofold longer than that using liquid electrolytes. In another study, Cui et al. in situ polymerized deep eutectic solvent-based polymer electrolyte (DES-PE) on the Li anode to endow as-fabricated LABs with a robust anodic interface.<sup>[133]</sup> The in situ formed DES-PE prevents the penetration of  $O_2$ ,  $N_2$ ,  $H_2O$ , and other gases in the ambient air, thus effectively protecting the Li anode and boosting the anodic reversibility.

The poor oxidation resistance of SPEs hinders their practical applications, especially under high working voltages in LABs. To address this concern, CSEs with high stability against oxidation have been extensively investigated,<sup>[134]</sup> which also have relatively higher  $Li^+$  conductivity and better thermal/chemical stability than SPEs. For instance, Zhou et al. substituted liquid electrolytes with a solid Li-ion conductor  $Li_{1.35}T_{1.75}Al_{0.25}P_{2.7}Si_{0.3}O_{12}$  (LTAP), serving as both a catholyte and a Li protector.<sup>[112]</sup> It effectively circumvents the decomposition of liquid electrolytes, growth of Li dendrites, and parasitic reactions with mixed gas phases of  $O_2$ ,  $H_2O$ , and  $CO_2$ , thereby enhancing the reversibility and cyclability of Li anodes. In a recent pioneering work, Yu et al. reported an integrated solid-state LAB using an ultrathin  $Li^+$ -exchanged zeolite X (LiX) membrane with high ionic conductivity as the solid electrolyte (Figure 6a).<sup>[76]</sup> This electrolyte is integrated with a cast Li anode and a carbon nanotube cathode through an in situ assembly process. Due to the inherent chemical stability of zeolite, the degradation of electrolytes by Li metal or air is efficiently inhibited.

Meanwhile, the ultra-slow dynamics of air penetration through LiXZM are favorable for impeding anodic corrosion. The Li metal protected by LiXZM was demonstrated to retain its metallic luster after 1000 h of ageing, revealing adequate protection from air erosion (Figure 6b). In addition, the by-products of  $\text{Li}_2\text{CO}_3$ ,  $\text{HCO}_2\text{Li}$ , and  $\text{CH}_3\text{CO}_2\text{Li}$  formed in conventional liquid electrolyte-based LABs are absent in the solid-state LAB using C-LiXZM. The mitigated electrolyte decomposition results in a more stable cycling performance of the LABs.

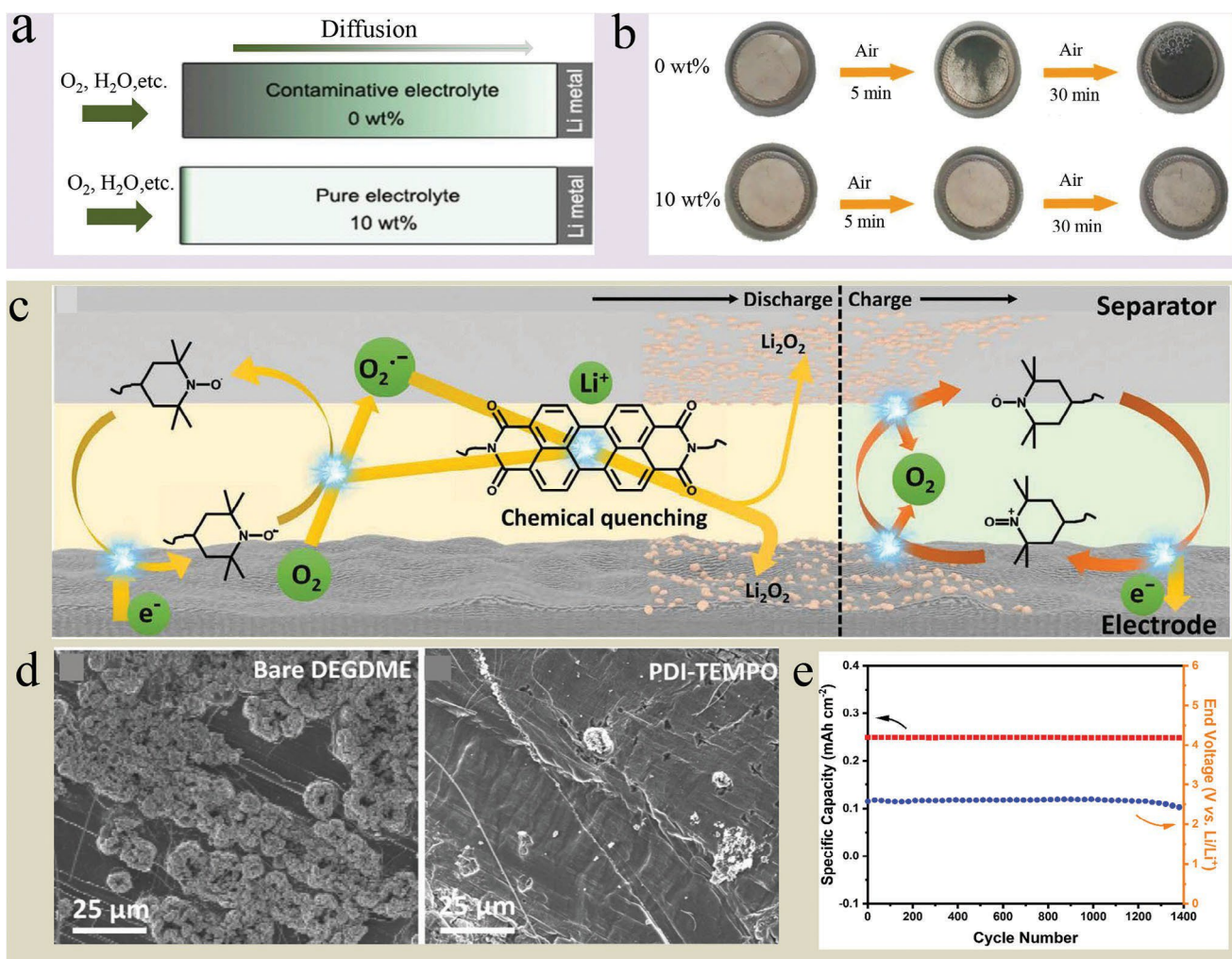


**Figure 4.** The use of anti-corrosion additive in liquid electrolytes for stabilizing the anode interfaces of LABs. a) Schematic representation of the anticorrosion effects of different electrolytes. (b) Optical images of the Li metal exposed to air after a different time soaking in 0 wt% HSCE and 10 wt% HSCE. Reproduced with permission.<sup>[119]</sup> Copyright 2020, Elsevier. c) The illustration of PDI-TEMPO to comprehensively suppress parasitic reactions. d) SEM images of the Li anodes from bare DEGDME electrolyte and PDI-TEMPO electrolyte after 10 cycles. e) The long-term cycling profile of Li– $\text{O}_2$  battery with 10 mm PDI-TEMPO electrolyte. Reproduced with permission.<sup>[47]</sup> Copyright 2022, AAAS.

Although considerable progress has been made in engineering solid-state electrolytes for high-performance LABs, the research in this field is still in its infancy. SPEs generally own poor oxidation resistance, while CSEs have limited ionic conductivity at room temperature. In addition, the poor interfacial contact between the Li anode and current CSEs is another major obstacle to obtaining reversible and durable LABs. One promising solution could be hybridizing CSEs and SPEs to integrate merits from both components toward improved (electro)chemical stability and reduced interface contact impedance.<sup>[135]</sup> Future research should be devoted to developing high-conductivity solid electrolytes with robust interfaces for next-generation LABs.

#### 4. Rational Design of Anode Structure/Composition

The uneven Li deposition at LAB anodes easily causes dendritic growth after repeated charging–discharging cycles, which may

penetrate the separator and result in subsequent internal short circuits and thermal runaway.<sup>[136-139]</sup> Moreover, the Li anode in LABs inevitably suffers from continuous deterioration because it is hyperreactive with H<sub>2</sub>O, O<sub>2</sub>, and the produced intermediates during charge–discharge. Therefore, it poses a high risk to the Li anode regarding structure collapse over prolonged cycles.<sup>[140-142]</sup> Structure modification and rational composition design can eliminate the corrosion of Li anodes, thus stabilizing the anodic interfaces. **Table 2** summarizes some recent advances based on anode alternatives to improve the performance of Li–air batteries. The following section will comprehensively review and discuss the typical methods reported, including artificial SEI construction and composite metal anode fabrication.

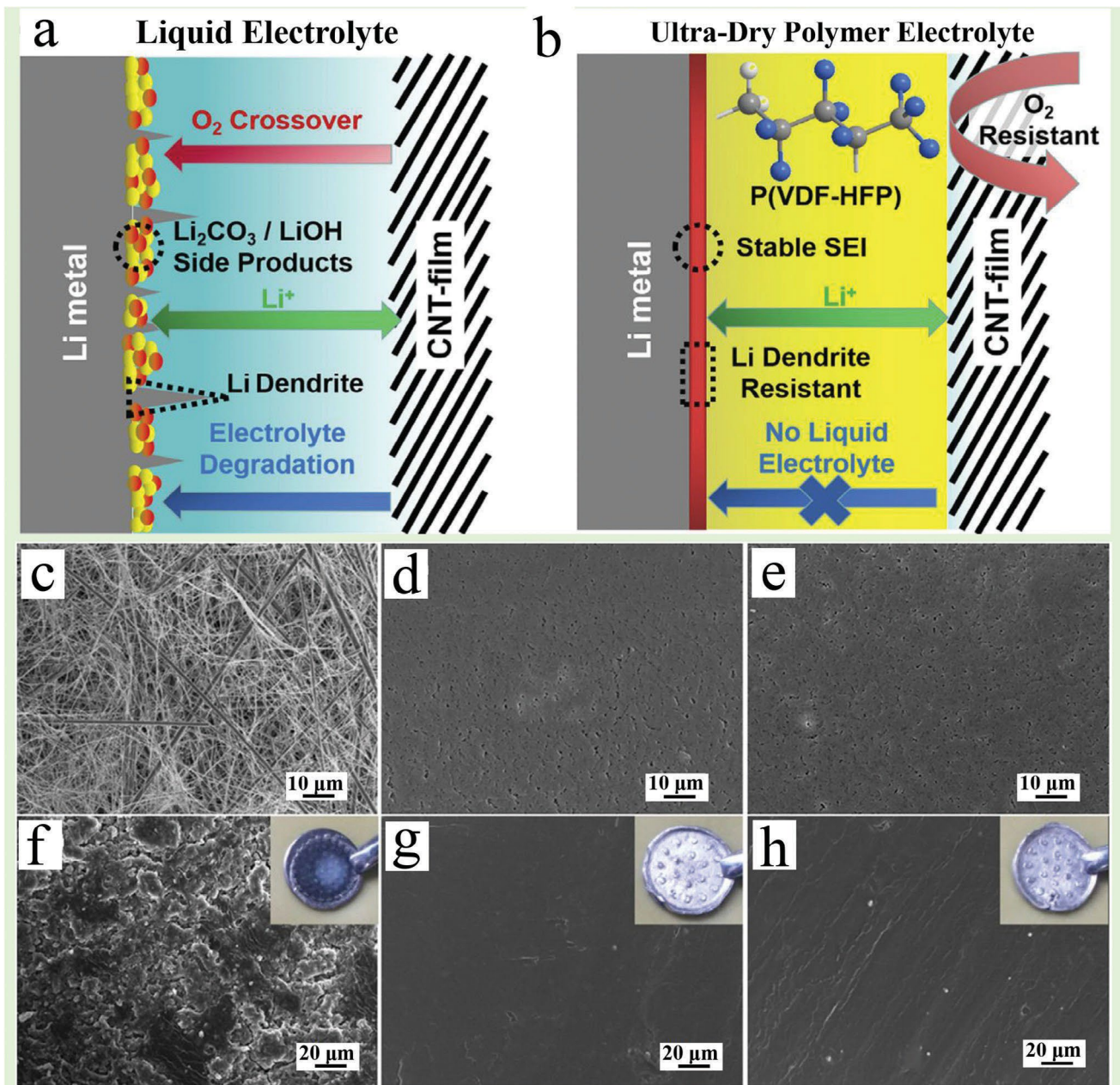


**Figure 5.** The construction of solid polymer electrolytes for stabilizing the anode interfaces of LABs. Schematic illustration of LABs with a) liquid electrolytes and b) UDPEs. SEM images of c) GF separator, d) PVDF membrane, e) P(VDF-HFP) membrane, and the surfaces of the Li anodes with f) GF, g) PVDF membrane, and h) P(VDF-HFP) membrane exposure to O<sub>2</sub> atmosphere for three days. Insets in (f–h) show the photographic images of the corresponding Li anode surfaces. Reproduced with permission.<sup>[132]</sup> Copyright 2020, Elsevier.

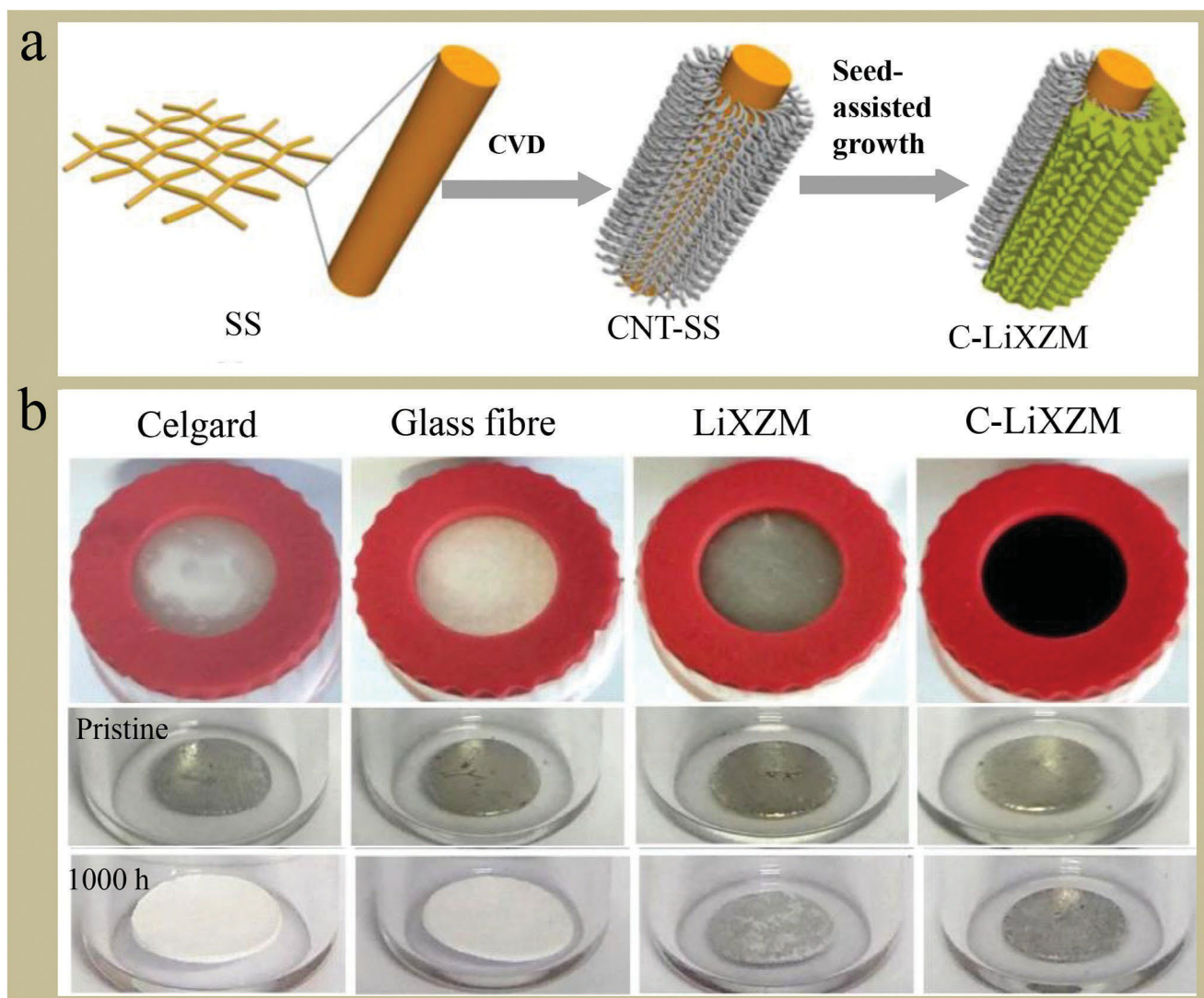


**Figure 6.** The construction of ceramic solid electrolytes for stabilizing the anode interfaces of LABs. a) Schematic of the design and preparation of the integrated C-LiXZM. b) Time-resolved optical images of Li metal inserted in the test devices sealed with Celgard separator (immersed with organic electrolyte), glass fiber separator (immersed with organic electrolyte), LiXZM, and C-LiXZM. Reproduced with permission.<sup>[76]</sup> Copyright 2021, Springer Nature.

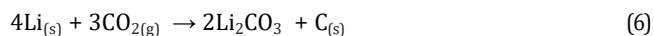
**Table 2.** Electrochemical performances of Li-air batteries with different anode and operation parameters.

Anode	Cycles	Capacity	Current density	Operating environment	Ref
Lithiated Al anode	100	1000 mAh g <sup>-1</sup>	100 mA g <sup>-1</sup>	O <sub>2</sub>	[52]
Li-Na alloy anode	140	1000 mAh g <sup>-1</sup>	200 mA g <sup>-1</sup>	O <sub>2</sub>	[53]
Lithium carbonate-protected Li anode	700	500 mAh g <sup>-1</sup>	500 mA g <sup>-1</sup>	Air	[90]
Porous graphene/Li anode	100	2000 mAh g <sup>-1</sup>	1000 mA g <sup>-1</sup>	O <sub>2</sub>	[143]
LiAl <sub>x</sub> -800-30 anode	400	1000 mAh g <sup>-1</sup>	0.2 mA cm <sup>-2</sup>	O <sub>2</sub>	[144]
Li <sub>x</sub> Si-CNT	20	0.66 mAh	/	O <sub>2</sub>	[145]
Lithiated hard carbon	75	/	0.08 mA g <sup>-1</sup>	O <sub>2</sub>	[146]
Li-SiO <sub>2</sub> /GO	348	1000 mAh g <sup>-1</sup>	1 A g <sup>-1</sup>	O <sub>2</sub>	[147]
I-containing polymer/alloy layer-based Li	120	1000 mAh g <sup>-1</sup>	500 mA g <sup>-1</sup>	Air	[148]
FEC-treated Li metal	>100	1000 mAh g <sup>-1</sup>	300 mA g <sup>-1</sup>	O <sub>2</sub>	[149]

#### 4.1. Constructing Artificial SEI Layer

The physicochemical properties of SEI play a critical role in determining the electrochemical performances, especially the cycling stability of the Li metal anode and the LABs.<sup>[150-152]</sup> Recent studies have suggested that crossover O<sub>2</sub> and H<sub>2</sub>O can corrode the native SEI formed at the Li anode surface from the open air.<sup>[124,153]</sup> Artificial SEI layers are functional thin films pre-constructed on the Li anode surface, generally impermeable to O<sub>2</sub> and H<sub>2</sub>O. Therefore, it can protect the Li anode from parasitic reactions with corrosive species, thereby improving the cycling stability of rechargeable LABs.<sup>[154-156]</sup>

In an early study, Osaka et al. extended the cycle life of Li anode in a CO<sub>2</sub>-saturated LiClO<sub>4</sub>/propylene carbonate electrolyte, in which the formation of Li<sub>2</sub>CO<sub>3</sub> at the Li metal surface inhibits dendritic Li deposition.<sup>[157]</sup> Recent research revealed the in-depth mechanism of the above anode protection through combined spectroscopic characterizations and theoretical simulations.<sup>[90]</sup> Such Li<sub>2</sub>CO<sub>3</sub>/C anode-protection coating can be directly conducted on a Li anode. In a custom-made electrochemical Li-CO<sub>2</sub> cell filled with pure CO<sub>2</sub>, a protective coating layer composed of nanorods was built on the Li metal surface after ten discharge-charge cycles (**Figure 7a**), based on the following reaction:



The phase composition was determined to be Li<sub>2</sub>CO<sub>3</sub>/C by Raman tests (**Figure 7b**). Density functional theory (DFT) calculations revealed that the Li<sub>2</sub>CO<sub>3</sub> layer endows a high energy barrier of 1.2–3.2 eV, thus effectively blocking the adsorption of N<sub>2</sub> and O<sub>2</sub> (**Figure 7c,d**). As a result, the Li<sub>2</sub>CO<sub>3</sub>-protected Li metal anodes show similar electrochemical properties in the air to those in pure oxygen (**Figure 7e**). Similarly, Huang et al. produced air-stable lithium spheres (ASLSs) with a Li core and Li<sub>2</sub>CO<sub>3</sub> shell through electrochemical Li plating under a CO<sub>2</sub> atmosphere.<sup>[158]</sup> The Li<sub>2</sub>CO<sub>3</sub> shell is highly hydrophobic and non-reactive with O<sub>2</sub> and N<sub>2</sub> in ambient air, protecting the Li core from corrosive species. Moreover, it has a good Li<sup>+</sup>-ion conductivity for rapid interfacial charge transfer.

Zhou et al. fabricated another organic-rich protective layer on the Li surface by facile chemical reactions between Li metal and 1,4-dioxacyclohexane (DOA), which is mainly composed of ethylene oxide monomers and functions as an efficient barrier to shield the Li metal anode.<sup>[48]</sup> Very recently, Cui et al. designed an iodine-containing polymer/alloy hybrid layer-based Li (IPA-Li) via the replacement reaction between zinc iodide (ZnI<sub>2</sub>) and Li and subsequent polymerization of ethyl  $\alpha$ -cyanoacrylate (**Figure 8a**).<sup>[148]</sup> The high mechanical flexibility of the polymer layer not only alleviates the internal stress at the Li surface but protects Li metal from O<sub>2</sub>/H<sub>2</sub>O attack, thus enabling durable storage of IPA-Li in the air (**Figure 8b**). The LiZn alloy nanoparticles offer many smooth Li<sup>+</sup>-conducting channels and afford a robust affinity with Li, which favors even Li nucleation and dendrite-free growth. The in situ differential electrochemical mass spectrometry (DEMS) tests revealed highly reversible charge storage in as-fabricated LAB dominated by O<sub>2</sub>-Li<sub>2</sub>O<sub>2</sub> conversion (**Figure 8c**) and therefore, a low voltage polarization during charge-discharge cycles (**Figure 8d**).

Despite the diversity and easiness of liquid-phase reactions with Li metal to produce artificial SEI layers, they are challenging to control, which generally produces loose and inhomogeneous films on Li surfaces. As a result, uneven Li deposition and undesirable side reactions may occur. To address this issue, Zhu and co-workers fabricated a self-eliminating passivated layer on the Li surface through facile evaporation of dichlorodimethylsilane (DCDMS).<sup>[153]</sup> The fresh Li dendrites formed in their infancy stage can be spontaneously eliminated by the Wurtz-type reaction with DCDMS because of their higher reactivity (**Figure 8e**). An as-generated protective layer is composed of alkali chloride and poly(dimethylsilylene), and it has multiple merits of high thermal stability, hydrophobicity, electrical insulation, and good Li<sup>+</sup>-ion conductivity. Moreover, the LAB with such passivated Li anodes exhibits high Coulombic efficiencies and a long cycling lifespan of over 200 cycles (**Figure 8f**). Likewise, Shao et al. proposed an effective strategy by immersing the Li metal anode in I<sub>2</sub> steam to create an artificial SEI (**Figure 8g**).<sup>[125]</sup> This ionically conductive LiI layer not only suppresses the growth of Li dendrites but alleviates the shuttle of RMs to the Li metal anode, thereby extending the cycle life of LABs (**Figure 8h,i**).

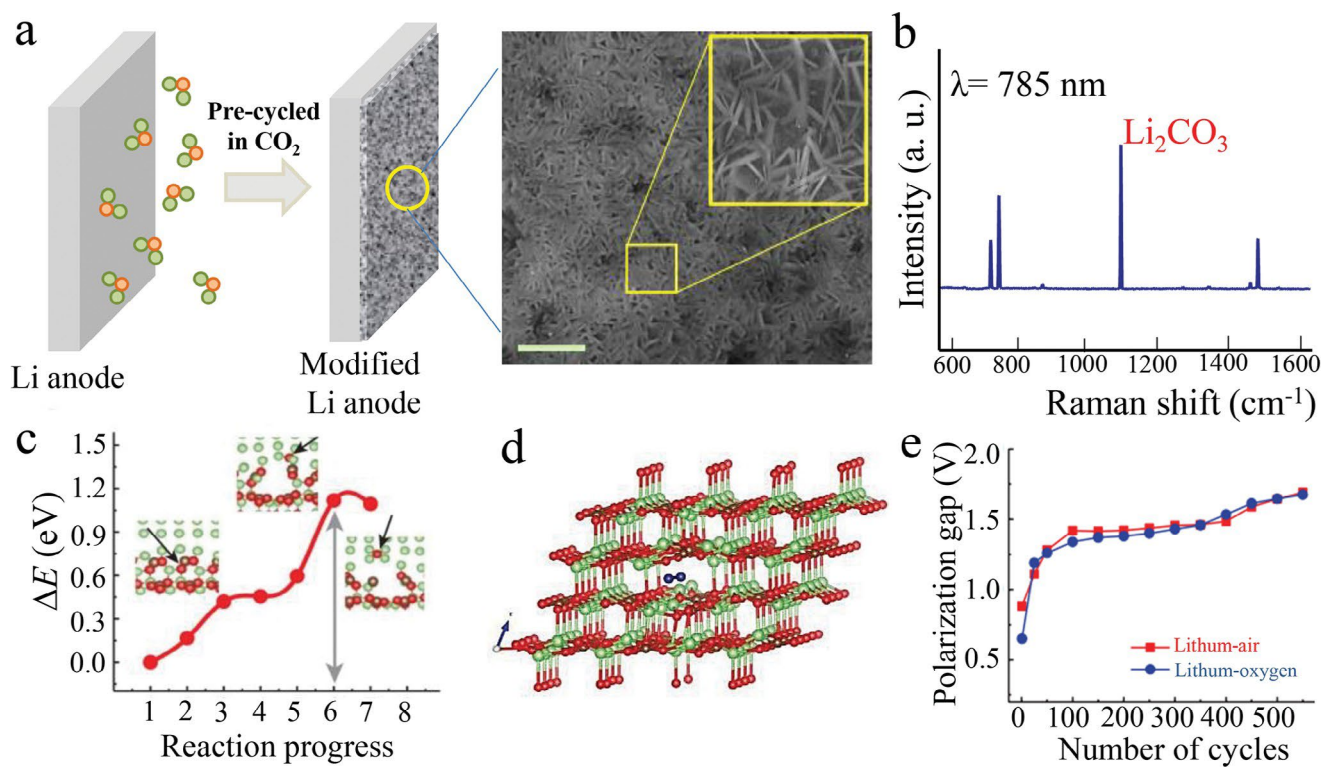


**Figure 7.** Constructing artificial SEI layers by pre-cycling the Li anode in  $\text{CO}_2$  for stabilizing the anode interfaces of LABs. a) Schematic of the synthesis process of  $\text{Li}_2\text{CO}_3/\text{C}$  layer (scale bar,  $1\ \mu\text{m}$ ). b) Raman spectra of the protected anode. c) Computational analysis revealed the cleavage of the C–O bond of  $\text{Li}_2\text{CO}_3$  at the interface and the migration of oxygen to the bulk Li (black arrows show the presence of oxygen). d) Computational analysis of  $\text{O}_2$  in a  $\text{Li}_2\text{CO}_3$ . e) The polarization gap between the lithium–air battery and the Li– $\text{O}_2$  battery under the same operating conditions. Reproduced with permission.<sup>[90]</sup> Copyright 2018, Springer Nature.

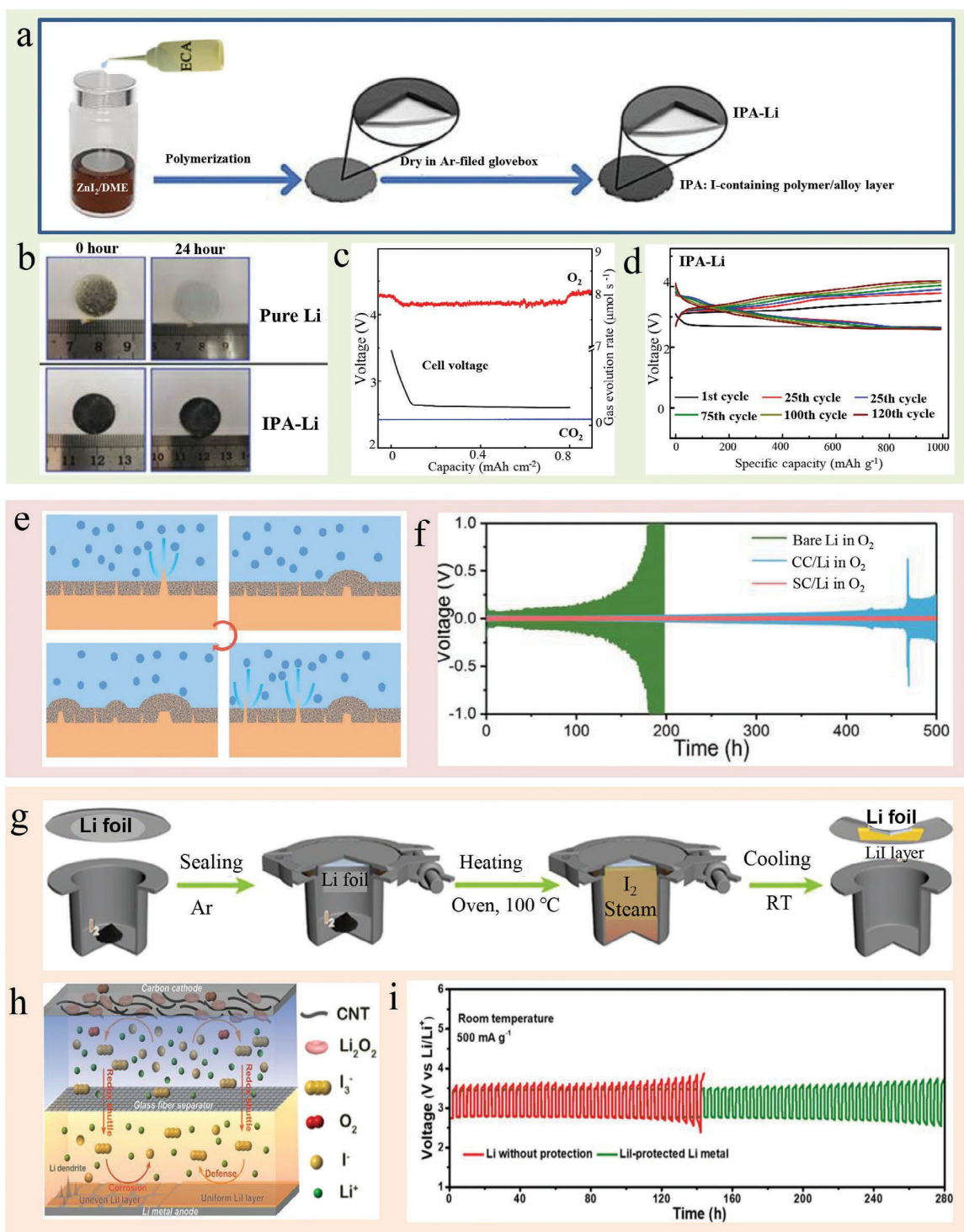


**Figure 8.** Constructing artificial SEI layers by chemical reactions for stabilizing the anode interfaces of LABs. a) Schematic of the synthesis process for the IPA-Li composite. b) Photograph images of the bare Li and IPA-Li anode exposed to the ambient air for various durations. c) The O<sub>2</sub> consumption/corresponding discharge curves. d) Voltage profiles under different cycles for IPA-Li-based LABs. Reproduced with permission.<sup>[148]</sup> Copyright 2021, Wiley-VCH GmbH. e) The schemes of Li deposit on SC/Li. f) Cycling performance of the symmetric Li batteries in O<sub>2</sub>. (CC/Li: Li metal with dichloro- propane (C<sub>3</sub>H<sub>6</sub>Cl<sub>2</sub>); SC/Li: Li metal reacts with LiCl/Poly(dimethylsilylene)). Reproduced with permission.<sup>[153]</sup> Copyright 2022, Wiley-VCH GmbH. g) Schematic illustration of the formation procedure of the protected Li metal. h) Shuttle mechanism and the function of the LiI protective layer. i) Cycling performance of the LABs. Reproduced with permission.<sup>[125]</sup> Copyright 2021, American Chemical Society.

## 4.2. Li-Containing Anode Design for Stabilizing the Interfaces

Artificial SEI forms a protective layer on the Li metal surface, which, however, does not change the inherent high (electro)chemical reactivity of Li metal anodes. The open system in LABs poses new challenges to the anodic interface stabilization except for uncontrollable Li deposition and drastic morphological changes of Li anodes in conventional Li-metal batteries.<sup>[159,160]</sup> Specifically, oxygen species of  $O_2^-/O_2^{2-}/^1O_2$  generated during charge-discharge are high nucleophilic radicals, which catalyze electrolyte decomposition to produce a variety of reactive byproducts.<sup>[80]</sup> Some other side products, such as LiOH,  $Li_2CO_3$ , and  $ROCO_2Li$ , are also continuously generated on the Li anode surface,<sup>[41,93]</sup> further deteriorating the interfacial stability.<sup>[161]</sup>

To stabilize the anodic interfaces, novel Li-containing anodes have been extensively studied recently. For example, Peng et al. developed a 3D network of carbon nanotubes (CNTs) cross-stacked layer by layer orthogonally. When applied in LABs, the cycle stability of this composite Li anode was greatly improved because of the dendrite-free Li deposition and stabilized SEI.<sup>[162]</sup> Similarly, another research group reported a Li-CNT composite anode with a self-assembled monolayer of octadecyl phosphonic acid as a tailor-designed SEI. The interwoven framework of CNTs was revealed to promote dendrite-free Li deposition within the 3D network without causing considerable volume expansion.<sup>[163]</sup> Moreover, the artificial SEI constructed on the Li-CNT composite surface restrains the parasitic side reactions between Li metal and the electrolyte.

Although the composite anodes own enhanced mechanical stability and reduced charge/discharge polarization, extending the life-cycle of Li anodes in LABs is still a great challenge because of their high (electro)chemical reactivity. To resolve this problem, lithium-alloying composites with lower reactivity, such as  $Li_xSn$ ,<sup>[164]</sup>  $LiAl_x$ ,<sup>[144]</sup>  $Li_xSi$ ,<sup>[165]</sup> and GaIn liquid metal anode<sup>[166]</sup> were exploited to replace Li metal. As a typical example, Zhou et al. developed a long-life Li-ion  $O_2$  battery based on commercial silicon particles for the first time.<sup>[167]</sup> Fluoroethylene carbonate (FEC) was introduced in a glyme-based electrolyte to produce a durable and deformable SEI film (Figure 9a). It comprises  $Li_2CO_3$ , LiF, organic species, and polyfluorocarbon, endowing the anode with strong resistibility toward oxygen crossover effects and boosting stable cycling capability (Figure 9b). However, the limited Li source in as-fabricated LABs makes it quite challenging to maintain a long lifespan even when good protection of the alloying composite anode from corrosion reaction is realized.

Besides Li-alloying anodes, recently Zhou's group proposed an organic liquid anode of biphenyl Li (Bp-Li) complex to replace the conventional solid-phase Li metal or Li-alloying anode.<sup>[168]</sup> When this liquid anode is utilized with a zeolitic imidazolate framework ZIF7 membrane as a separator, the notorious issues associated with Li metal anodes are well addressed (Figure 9c). Bp-Li works as a stable negative electrode at the anode side. The reactivity of Bp-Li with moisture was also studied by dropping  $H_2O$  into it, and the results in Figure 9d demonstrate its high resistance to  $H_2O$  corrosion. The ZIF-7 serves as an interlayer bridging the cathode and anode sides from the following three aspects: 1) conducting the  $Li^+$  ions during charge/discharge; 2) preventing the BP-Li liquid anode from shuttling to the  $O_2$  cathode and causing short circuits; 3) constraining RMs at the anode side to get rid of their crossover. Moreover, as-fabricated organic  $O_2$  batteries with Bp-Li anode show a superior rate performance, which benefits from the high electronic/ionic conductivity of Bp-Li and rapid  $Li^+$  ion transporting capability. It also delivers a high reversible specific capacity of  $2000 \text{ mAh g}^{-1}$  at a high current density of  $4000 \text{ mA g}^{-1}$  for 100 cycles (Figure 9d).

In summary, recent progress on the rational design of Li anode structure/composition toward alleviated corrosion reaction and stabilized anodic interface has been critically reviewed. Artificial SEI layers impermeable to  $O_2$  and  $H_2O$  can protect the Li anode from parasitic reactions. 3D composite Li enables enhanced mechanical stability and reduced charge/discharge polarization, while other Li-containing anodes, including Li-alloying composite and liquid organic anodes, own lower (electro)chemical reactivity. Despite these advances, there are still numerous challenges to be overcome. Current artificial SEI can only protect the Li anode from the attack of single gas or corrosive species, and multifunctional protective SEI layers are required to inhibit the crossover corrosion. 3D composite Li anodes possess high reactivity and thus poor resistance to corrosion reactions. Li-alloying composites own limited Li source and therefore short lifespan, and liquid organic anodes are exposed to increased risks of cathode/anode contact and subsequent short circuits. Novel Li-containing anodes with smart compositions/structures are urgently needed for future stable AMABs.

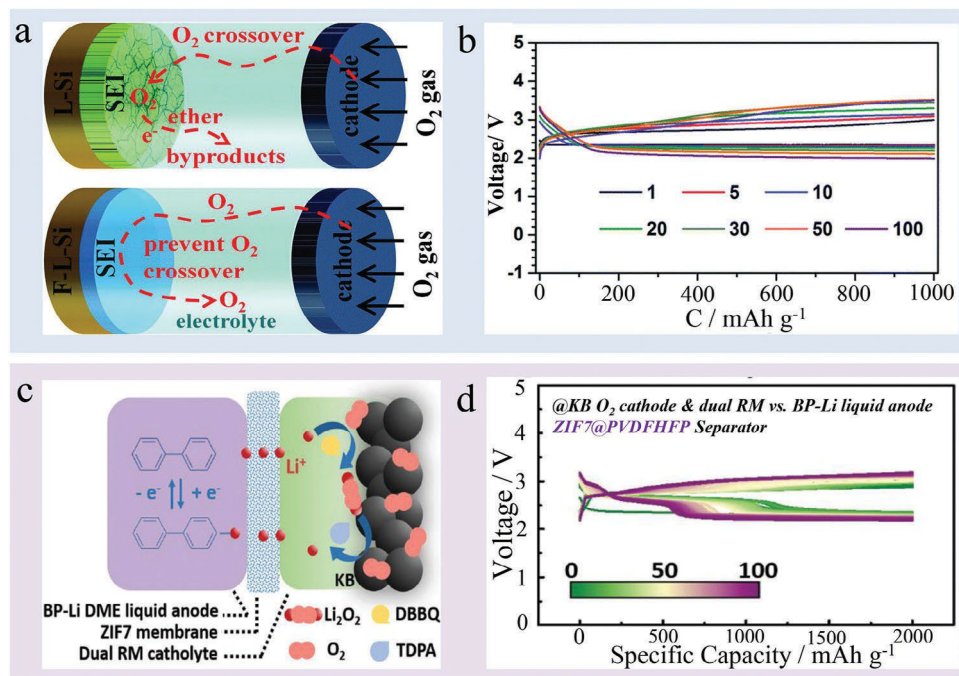


**Figure 9.** Design of Li-containing anodes for stabilizing the anode interfaces of LABs. a) SEI film evolution of L-Si and F-L-Si anodes. b) The discharge/charge curves of LABs with F-L-Si anodes. Reproduced with permission.<sup>[167]</sup> Copyright 2020, 2016, The Royal Society of Chemistry. c) The schematic of the organic BP-Li-O<sub>2</sub> battery. d) Cycling performance of organic O<sub>2</sub> batteries. Reproduced with permission.<sup>[168]</sup> Copyright 2020, Wiley-VCH GmbH.

## 5. Design of Functional Separators

A separator is a permeable membrane placed between the cathode and the anode in LABs, used to prevent internal short circuits of cells while allowing smooth transportation of ionic charge carriers.<sup>[169]</sup> Conventional separators in LABs are porous polymeric membranes such as polyethylene (PE) or polypropylene (PP), incapable of suppressing the crossover of atmospheric gases and corrosive RMs from the cathode side.<sup>[57,58,170,171]</sup> In recent years, hazardous gases/RMs-blocking functional separators have been exploited to protect the Li anode in LABs.<sup>[172]</sup> For example, Choi et al. developed a poreless polyurethane (PU) separator in LABs, which prevents H<sub>2</sub>O and O<sub>2</sub> from infiltrating and gaining access to the Li anode

surface while allowing Li<sup>+</sup> ions to diffuse through selectively (Figure 10a).<sup>[57]</sup> The Li<sup>+</sup> mobility was largely promoted due to the hydrophilic interaction between the electrolyte and the polar functional groups (Figure 10b). Due to the improved anodic interfacial stability, the LAB with the PU separator exhibited greatly improved cycling performance (Figure 10c). Similarly, Zhang et al. in situ fabricate a stable tissue-directed/reinforced bifunctional separator/protection film (TBF) on the surface of lithium metal.<sup>[170]</sup> The TBF layer has excellent chemical, electrochemical, and mechanical stability. It effectively protects Li from the corrosion of oxygen species, moisture, and electrolytes, resulting in excellent anode reversibility.

RMs can facilitate the oxidation of Li<sub>2</sub>O<sub>2</sub> toward reduced over-potential during charging,<sup>[35,93,113]</sup> yet they might also seriously degrade the Li metal anode through parasitic reactions.<sup>[171]</sup> A proper separator design has been proposed to confine the RMs and avoid their shuttling attack on the Li metal anode. For instance, Sun et al. coated a polymer mixture of poly(3,4-ethylene dioxythiophene) (PEDOT) and polystyrene sulfonate (PSS) on the commercial glass fiber separator. Its robust Coulombic interaction with RMs effectively suppresses their migration toward the Li metal anode.<sup>[173]</sup> Wen et al. reported the inhibition of I<sub>3</sub><sup>-</sup> shuttling in LiI-involved LABs.<sup>[174]</sup> A mixture of MXene nanosheets and bacterial cellulose (BC) nanofibers were loaded onto the glass fiber (GF) membrane (Figure 10e). The -OH functional groups on MXene surfaces served as efficient binding sites to restrain the I<sub>3</sub><sup>-</sup> shuttling, and the three-dimensional porous architecture facilitated rapid Li<sup>+</sup> transfer. As a result, the Li anode stability was enormously improved, and the fabricated LAB exhibited a stable cycle life of up to 100 cycles (Figure 10f).

Despite these progresses in developing advanced separators for suppressing corrosive gas/RM shuttling, current separators are mostly single-functional and cannot provide comprehensive protection. Moreover, the limited number of active sites for the physicochemical adsorption of gas phases/RMs, as well as the difficulty in their sustainable functioning over prolonged charge-discharge cycles, greatly hinder their practical applications. Future development of multifunctional and durable separators in AMABs is highly desirable.

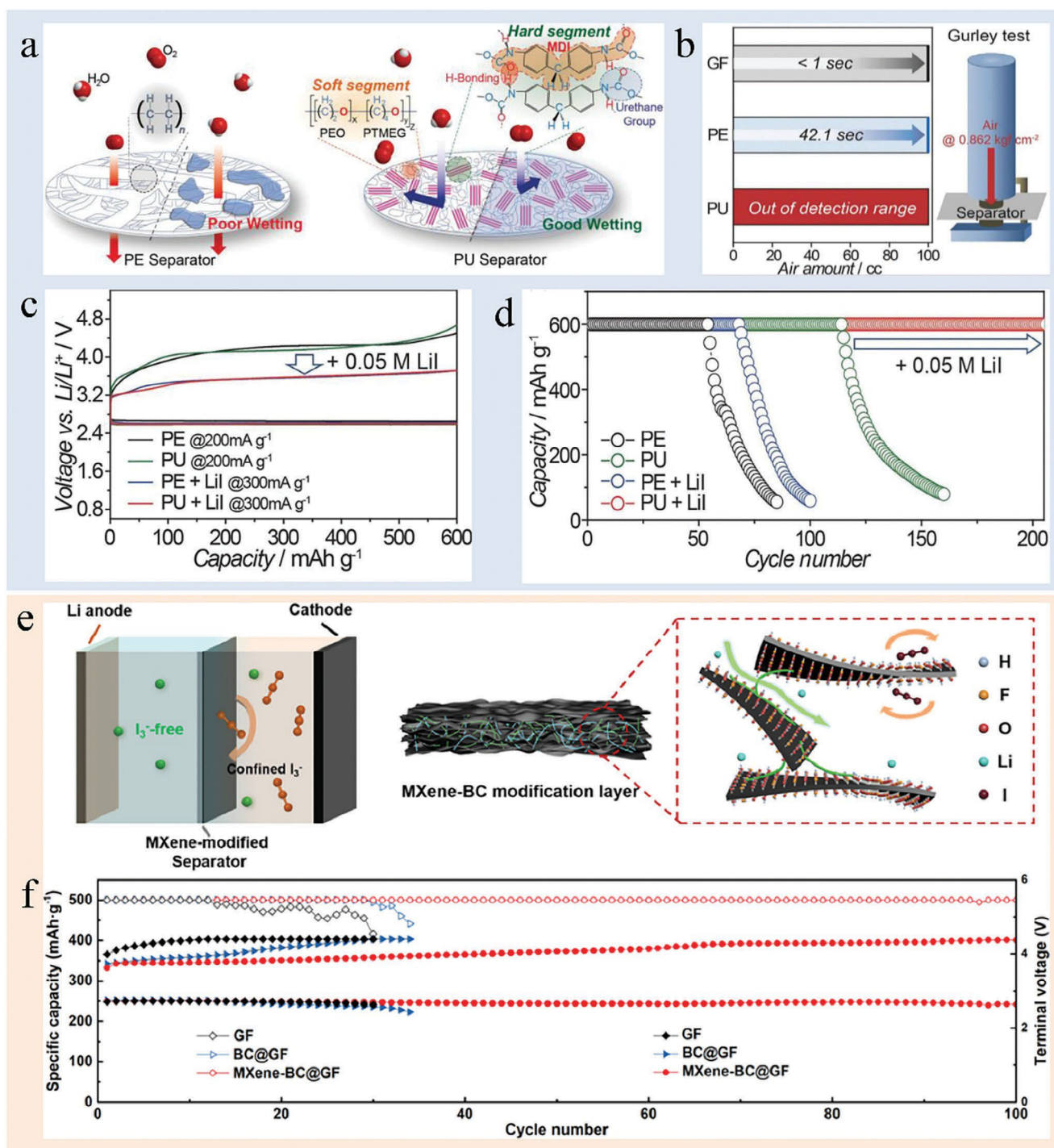


**Figure 10.** The design of functional separators for stabilizing the anode interfaces of LABs. a) Illustration of the separator effect on electrolyte wetting and gas/water permeation. b) The air permeability results of various separators. c,d) The cycling performance of PE, PU, PE+LiI, and PU+LiI cells. Reproduced with permission.<sup>[57]</sup> Copyright 2016, Wiley-VCH GmbH. e) Schematic illustration of suppressing  $\text{I}_3^-$  shuttling with the MXene-modified separator in LABs. f) Terminal discharge voltage of different separators. Reproduced with permission.<sup>[174]</sup> Copyright 2021, American Chemical Society.

## 6. Anode Interface Stabilization in Na/K–Air Batteries

Na/K–air batteries (NABs/KABs) have been considered promising alternatives to LABs for large-scale energy storage applications because of the low cost and abundant resources of Na/K, as well as quite similar electrochemical properties to the Li

counterparts.<sup>[175-178]</sup> Nevertheless, the hyperactive Na and K metals are more vulnerable in the atmospheric environment, making it considerably more challenging to handle the aforementioned difficulties in anodic interface stabilization.<sup>[178,179]</sup> Numerous pioneering works have been reported in recent years for developing durable NAB/KAB anodes, among which representative progresses are summarized as follows.

To enable efficient Na plating/stripping in an oxygenated environment, Zhou and co-workers pre-cycled the Na metal anode in the functional electrolyte containing 2 wt% fluoroethylene carbonate (FEC).<sup>[180]</sup> After the preferential reduction of FEC, a durable artificial SEI film rich in NaF has been produced on the tailored Na ( $T_{Na}$ ) anode, which can efficiently suppress the  $O_2$  crossover and undesirable side reactions (**Figure 11a**). As-constructed NABs with  $T_{Na}$  anodes maintain stable cycling for over 300 h in  $O_2$ , while pristine Na ( $P_{Na}$ ) anodes were short-circuited after 230 h (Figure 11b,c).

Kang et al. developed a liquid Na–K alloy anode for constructing dendrite-free KABs (Figure 11d).<sup>[181]</sup> The liquid anode provides a homogeneous and robust liquid–liquid anode–electrolyte interface, rendering superior stability to the traditional solid–liquid interface. DFT calculations revealed the less favorable interaction of diethylene glycol dimethyl ether (DEGDME) solvents on the Na–K alloy surface (Figure 11e). Therefore, it facilitates uniform K plating/stripping and subsequently helps address the safety concerns derived from the dendrite growth.

Wu et al. developed a freestanding 3D sulfur-doped porous graphene network as a reactive armor to protect the K metal anode.<sup>[75]</sup> The sulfur dopants in the graphene matrix react with the crossover species like dissolved  $O_2$  and superoxide anions ( $O_2^-$ ) to form anionic sulfonates/sulfates, which could serve as active sites for preferential nucleation and growth of  $KO_2$  (Figure 11f). The produced  $KO_2$  layer on the graphene surface protects the crossover oxygen species from etching the inner fresh K metal. (Figure 11g,h). Consequently, the as-constructed K– $O_2$  battery with the protected K anode realizes a boosted lifespan of 140 stable cycles, three times longer than that of the K– $O_2$  battery with the bare K anode (Figure 11i).

Despite the progress achieved, most of them utilized pure oxygen in the cathode, resulting in sacrificed gravimetric/volumetric energy densities.<sup>[182]</sup> The study on stabilizing Na/K anodes in an open environmental atmosphere of NABs/KABs is still in its infancy. Challenges remain in resolving the issues caused by the high chemical reactivity of Na/K–metal interfaces and the uncontrollable morphology evolution of the Na/K anodes. The construction of in situ/ex situ protective films on the Na/K anode surfaces and the development of alternative anode materials with higher stability and reversibility are greatly desired.

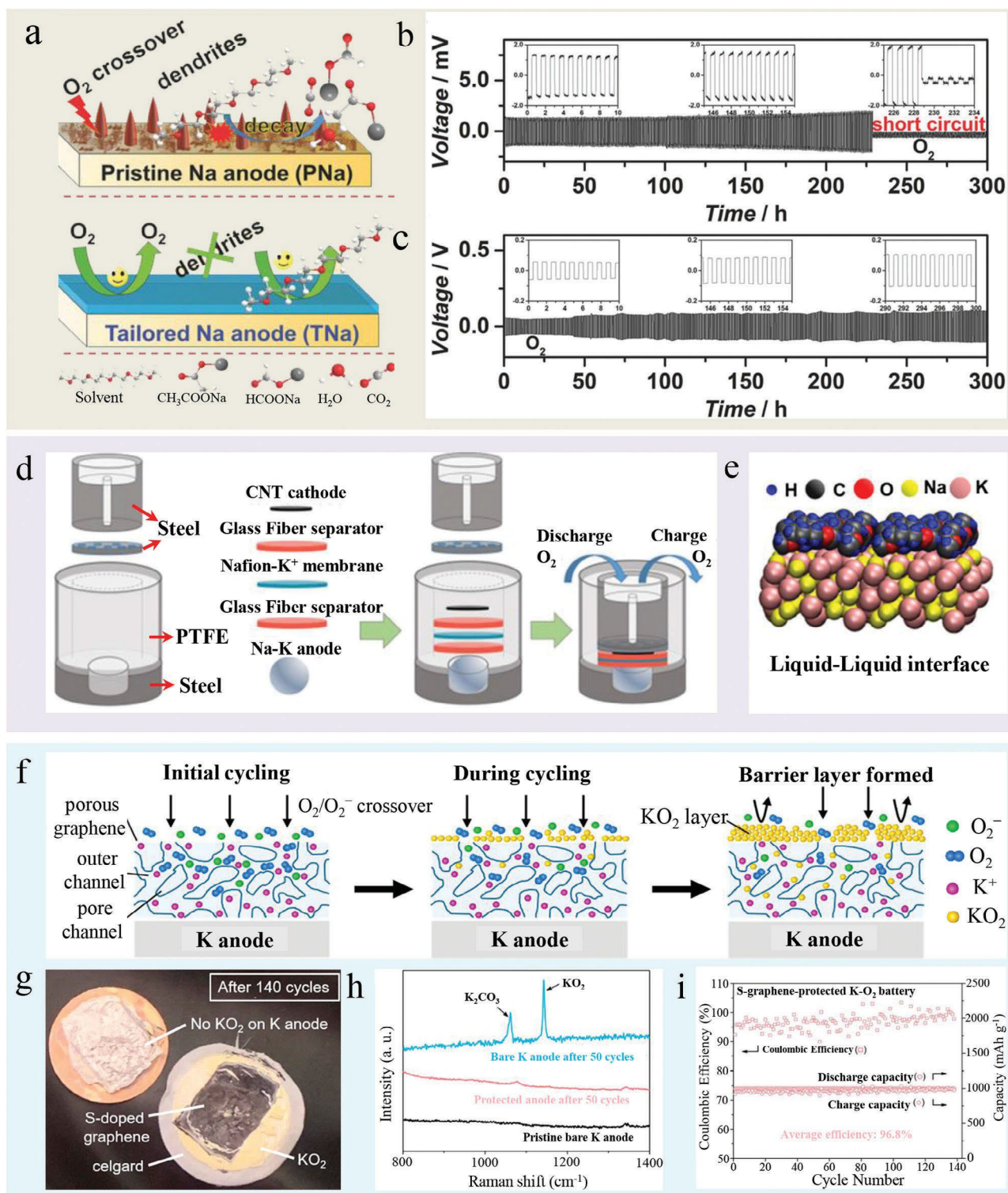


**Figure 11.** Examples for the stabilization of anode interfaces in Na/K-air batteries. a) Illustration of problems on pristine Na anode (PNa) in Na-O<sub>2</sub> battery and illustration of improvements on T<sub>Na</sub>. b,c) The effective resistivity of T<sub>Na</sub> against O<sub>2</sub> crossover. Reproduced with permission.<sup>[180]</sup> Copyright 2018, Wiley-VCH GmbH. d) K-O<sub>2</sub> battery configuration based on the Na-K liquid alloy as the anode. e) Lowest energy configuration of a fully covered Na<sub>4</sub>K<sub>5</sub> surface with DEGDME solvents. Reproduced with permission.<sup>[181]</sup> Copyright 2017, American Chemical Society. f) Schematic illustration of KO<sub>2</sub> barrier layer on the S-doped porous graphene outer surface. g) S-graphene-protected K anode after 140 cycles (graphene peeled off). h) Raman spectra of different anodes after 140 cycles. i) Cyclability of the S-graphene-protected K-O<sub>2</sub> battery. Reproduced with permission.<sup>[75]</sup> Copyright 2020, American Chemical Society.

## 7. Conclusions and Perspectives

AMABs hold great promise for next-generation electrochemical energy storage because of their ultra-high energy densities. However, the complicated side reactions involved at the solid-liquid-gas triple-phase interface of the anode are formidable challenges to achieve reversible and durable metal anodes, which become a bottleneck hindering the practical applications of AMABs. In this timely review, we have critically summarized the major issues associated with the triple-phase anodic interface of AMABs, including 1) the crossover of mixing gas phases/RMs and subsequent severe parasitic reactions with the metallic anode; 2) the interference of the  $O_2$  electrochemistry by reactive oxygen intermediates ( $O_2^-$ ,  $O_2^{2-}$ , and  $^1O_2$ ); 3) the deterioration of uneven metal deposition and SEI inhomogeneities. Various strategies developed to mitigate the above challenges have been comprehensively reviewed, mainly including 1) novel liquid/solid electrolyte formulation; 2) artificial SEI construction on metal anodes and Li-containing anode design; and 3) functional separator modification. These efforts have greatly improved the stability of the anode interface in AMABs.

Despite these advances, the development of stable metal anodes in AMABs is still in its infancy before the following concerns are well tackled. i) Most liquid electrolytes developed so far have the singular function of either forming native protective SEI or boosting the intrinsic anti-corrosion capability, but the improvement of anode reversibility is far from satisfactory. Their evaporation/leakage in the open system poses another severe concern against sustainable battery operation. ii) Integrated design of solid electrolytes and metal anodes enabling effective interfacial contact remains a significant challenge. iii) The constructed artificial SEI layer on the metal anode shows a limited thickness and thus decelerates the ion transfer kinetics and deteriorates the electrochemical performance of AMABs. Moreover, it's still a great challenge to achieve controllable and scalable preparation of artificial SEI on highly reactive alkali metal anodes. iv) Rational design of the anode structure/composition like 3D composite Li and Li-containing compounds cannot fully eliminate the attacks by corrosive gases/intermediates/RMs; v) It is extremely difficult to develop multifunctional separators to effectively shield corrosive gas/RM toward sustainable operation of AMABs.

The electrochemical processes involved at anode interfaces are complicated and highly interrelated, making it unlikely to address all the above challenges by regulating individual components. Stabilizing the anodic interfaces is thus expected to be achieved from a systems engineering perspective. We present potential future research directions toward more durable metal anodes in AMABs as follows (Figure 12).

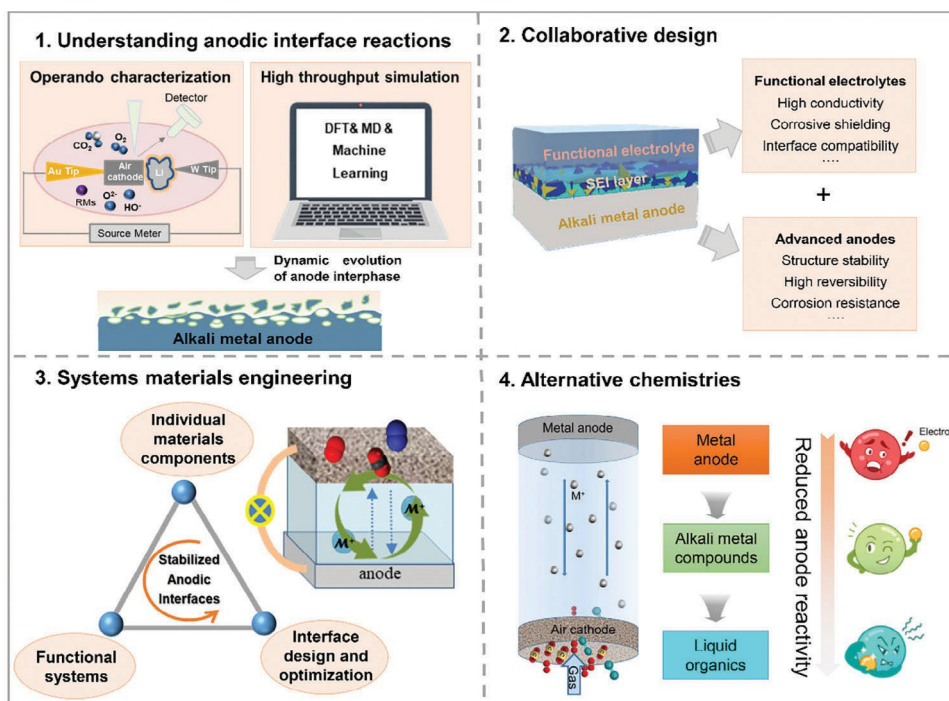


Figure 12. Outlook for the development of high-performance AMABs in the future.

- 1) *A more accurate understanding of the reaction mechanism at an-ode interfaces.* Although many studies have uncovered the underlying interfacial reaction mechanism of metal anodes in a single O<sub>2</sub> atmosphere, that under an open atmosphere with mixed gases is much more complicated and yet to be revealed. Consequently, gaining a sophisticated understanding of metal anode degradation in the real working environment is highly desirable. The development of advanced experimental techniques and multiscale modeling methods is urgently needed. A recent study has revealed the correlation between the morphological evolution of the Li anode and the electrochemical performance of LOBs by complementary X-ray and neutron tomography.<sup>[97]</sup> Cutting-edge operando characterization techniques, such as low-dose TEM imaging and X-ray computed tomography, allow direct probing of real-time electrochemical reactions at varying temporal and spatial scales. Further, by coupling with multiscale modeling methods like DFT, molecular dynamics (MD), and machine learning, a more accurate understanding of the reaction pathway and the composition evolution of electrolyte components/metal anodes/oxygen species during charge/discharge can be established. As such, more potential strategies can be proposed to precisely regulate/stabilize the an-odic interfaces.
  - 2) *A collaborative design of advanced electrolytes and anodes.* It is essential to consider the anode and electrolyte as an entity for achieving optimal components, microstructure, and electrochemical properties of anodic interfaces. By adopting such a holistic design approach, we can ensure that the resulting interface is well-suited to the specific requirements of the AMAB system with improved functionality and reliability. For instance, the rationally structured metal anodes coupled with properly formulated electrolytes allow the dynamic formation of protective SEI layers, enabling homogenized metal deposition and continuously alleviated interfacial parasitic reactions. The integrated design of the alkali metal anode and solid electrolyte can improve the interfacial contact and facilitate the interfacial charge transfer process in solid-state AMABs. More future re- search efforts are expected to be devoted to the synergistic optimization of the anode structure/composition and electrolyte formulation, which will more effectively stabilize the anodic interface, thus boosting the lifespan of AMABs.
  - 3) *Systems materials engineering for stabilizing the anodic interfaces.* Examining separated components is insufficient to address the scientific and technological challenges of the complicated AMAB system. Great attention should be drawn to investigating the interfaces between individual components. Systems materials engineering integrating individual components into an entire and functioning system can thus be far more effective for stabilizing the anode interfaces.<sup>[183]</sup> The pioneering work by Yu et al. has constructed an integrated cathode–electrolyte–anode system with well-defined interfaces, providing a more coherent continuum among the anode, electrolyte, and cathode.<sup>[76]</sup> Such a comprehensive system-level design is expected to help address all challenges confronting AMABs. Therefore, after the whole cell system is evaluated as an entirety and practical performance indicators are considered, it will pave the way for their large-scale applications.<sup>[184]</sup>
  - 4) *Exploration of alternative chemistries for more durable anodes in AMABs.* The investigation of new chemistries is expected to mitigate the stability challenges of anodic interfaces in AMABs. Replacing Li metal anodes based on Li plating/stripping with Li-containing compound anodes based on Li intercalation<sup>[185]</sup> or conversion reaction<sup>[74]</sup> could achieve improved safety, fast kinetics, and high reversibility while maintaining the low redox potential. Sealed rechargeable lithium–lithium oxide battery<sup>[186]</sup> based on reversible interconversion between super-oxide (LiO<sub>2</sub>) and lithium peroxide (Li<sub>2</sub>O<sub>2</sub>) can avoid the use of gas-phase cathodes, simplifying the triple-phase interface in conventional AMABs, thus significantly alleviating the difficulty in stabilizing the anode interface. These new battery systems can therefore mitigate the degradation of cathodes, decomposition of electrolytes, and corrosion of metal anodes toward more durable AMABs. Research works in this area are in their very early stages, and more innovative efforts and designs are highly required.
- Based on previously reported results and the above discussions, we conclude that there are no “one for all” strategies to address all challenges associated with the triple-phase interface of anode in AMABs. The individual components should be collaboratively designed in a systems engineering manner. While it is critical to accurately understand the reaction mechanism at anode interfaces, the investigation of new materials and new chemistries is highly encouraged. Despite numerous scientific and technological issues, this perspective is expected to provide guidelines to clarify the relationships among material composition/property, anodic interfacial behavior, and battery performance in the open system for rationally designing practical next-generation AMABs.

## Acknowledgements

The authors gratefully acknowledge financial support from The Hong Kong Polytechnic University (ZZLM, YY5K), Local Science and Technology Development Project of the Central Government (No. 2022ZY0011), Natural Science Foundation of Guangdong (No. 2023A1515010020), Innovation and Technology Fund (ITS-325-22FP). Q.L. thanks the financial support from the Natural Science Foundation of Jiangxi Province (No. 20232ACB214001), the Research fund from Jingxi Province Human Resources and Social Security Department, and the Chinese Academy of Sciences. Q.-H.Y. is grateful to the National Natural Science Foundation of China (No. 51932005).

## Conflict of Interest

The authors declare no conflict of interest.

- [1] J. M. Tarascon, M. Armand, *Nature* **2001**, *414*, 359.
- [2] P. G. Bruce, *Solid State Ionics* **2008**, *179*, 752.
- [3] P. G. Bruce, B. Scrosati, J.-M. Tarascon, *Angew. Chem., Int. Ed.* **2008**, *47*, 2930.
- [4] M. Li, J. Lu, Z. Chen, K. Amine, *Adv. Mater.* **2018**, *30*, 1800561.
- [5] J. B. Goodenough, K.-S. Park, *J. Am. Chem. Soc.* **2013**, *135*, 1167.
- [6] P. G. Bruce, S. A. Freunberger, L. J. Hardwick, J.-M. Tarascon, *Nat. Mater.* **2012**, *11*, 19.
- [7] B. Ge, Y. Sun, J. Guo, X. Yan, C. Fernandez, Q. Peng, *Small* **2019**, *15*, 1902220.
- [8] D. Li, H. Zhou, *Mater. Today* **2014**, *17*, 451.
- [9] A. Van der Ven, J. Bhattacharya, A. A. Belak, *Acc. Chem. Res.* **2013**, *46*, 1216.
- [10] Z.-L. Wang, D. Xu, J.-J. Xu, X.-B. Zhang, *Chem. Soc. Rev.* **2014**, *43*, 7746.
- [11] P. Tan, W. Kong, Z. Shao, M. Liu, M. Ni, *Prog. Energy Combust. Sci.* **2017**, *62*, 155.
- [12] S. C. Jesudass, S. Surendran, J. Y. Kim, T.-Y. An, G. Janani, T.-H. Kim, J. K. Kim, U. Sim, *Electrochem. Energy R.* **2023**, *6*, 27.
- [13] Y.-C. Lu, B. M. Gallant, D. G. Kwabi, J. R. Harding, R. R. Mitchell, M. S. Whittingham, Y. Shao-Horn, *Energy Environ. Sci.* **2013**, *6*, 750.
- [14] Z.-L. Wang, D. Xu, J.-J. Xu, L.-L. Zhang, X.-B. Zhang, *Adv. Funct. Mater.* **2012**, *22*, 3699.
- [15] H. Wang, X. Wang, M. Li, L. Zheng, D. Guan, X. Huang, J. Xu, J. Yu, *Adv. Mater.* **2020**, *32*, 2002559.
- [16] K. Surya, M. S. Michael, S. R. S. Prabaharan, *Solid State Ionics* **2018**, *317*, 89.
- [17] J. Lu, L. Li, J.-B. Park, Y.-K. Sun, F. Wu, K. Amine, *Chem. Rev.* **2014**, *114*, 5611.
- [18] D. Geng, N. Ding, T. S. A. Hor, S. W. Chien, Z. Liu, D. Wu, X. Sun, Y. Zong, *Adv. Energy Mater.* **2016**, *6*, 1502164.
- [19] X. Bi, K. Amine, J. Lu, *J. Mater. Chem. A* **2020**, *8*, 3563.
- [20] J. Lu, Y. Jung Lee, X. Luo, K. Chun Lau, M. Asadi, H.-H. Wang, S. Brombosz, J. Wen, D. Zhai, Z. Chen, D. J. Miller, Y. Sub Jeong, J.-B. Park, Z. Zak Fang, B. Kumar, A. Salehi-Khojin, Y.-K. Sun, L. A. Curtiss, K. Amine, *Nature* **2016**, *529*, 377.
- [21] D. Zhai, K. C. Lau, H.-H. Wang, J. Wen, D. J. Miller, J. Lu, F. Kang, B. Li, W. Yang, J. Gao, E. Indacochea, L. A. Curtiss, K. Amine, *Nano Lett.* **2015**, *15*, 1041.
- [22] L. Luo, B. Liu, S. Song, W. Xu, J.-G. Zhang, C. Wang, *Nat. Nanotechnol.* **2017**, *12*, 535.
- [23] L. Liu, Y. Liu, C. Wang, X. Peng, W. Fang, Y. Hou, J. Wang, J. Ye, Y. Wu, *Small Methods* **2022**, *6*, 2101280.
- [24] C. Shu, J. Wang, J. Long, H.-K. Liu, S.-X. Dou, *Adv. Mater.* **2019**, *31*, 1804587.
- [25] Y. Zhang, Q. Cui, X. Zhang, W. C. McKee, Y. Xu, S. Ling, H. Li, G. Zhong, Y. Yang, Z. Peng, *Angew. Chem., Int. Ed.* **2016**, *55*, 10717.
- [26] Y. Li, X. Wang, S. Dong, X. Chen, G. Cui, *Adv. Energy Mater.* **2016**, *6*, 1600751.
- [27] B. D. McCloskey, D. S. Bethune, R. M. Shelby, G. Girishkumar, A. C. Luntz, *J. Phys. Chem. Lett.* **2011**, *2*, 1161.
- [28] S. A. Freunberger, Y. Chen, Z. Peng, J. M. Griffin, L. J. Hardwick, F. Bardé, P. Novák, P. G. Bruce, *J. Am. Chem. Soc.* **2011**, *133*, 8040.
- [29] M. M. Ottakam Thotiyil, S. A. Freunberger, Z. Peng, Y. Chen, Z. Liu, P. G. Bruce, *Nat. Mater.* **2013**, *12*, 1050.
- [30] J. Xie, X. Yao, Q. Cheng, I. P. Madden, P. Dornath, C.-C. Chang, W. Fan, D. Wang, *Angew. Chem., Int. Ed.* **2015**, *54*, 4299.
- [31] F. Li, M.-L. Li, H.-F. Wang, X.-X. Wang, L.-J. Zheng, D.-H. Guan, L.-M. Chang, J.-J. Xu, Y. Wang, *Adv. Mater.* **2022**, *34*, 2107826.
- [32] B. Ge, J. Wang, Y. Sun, J. Guo, C. Fernandez, Q. Peng, *ACS Appl. Energy Mater.* **2020**, *3*, 2789.
- [33] D. M. Itkiss, D. A. Semenenko, E. Y. Kataev, A. I. Belova, V. S. Neudachina, A. P. Sirotina, M. Hävecker, D. Teschner, A. Knop-Gericke, P. Dudin, A. Barinov, E. A. Goodilin, Y. Shao-Horn, L. V. Yashina, *Nano Lett.* **2013**, *13*, 4697.
- [34] X. Gao, Y. Chen, L. Johnson, P. G. Bruce, *Nat. Mater.* **2016**, *15*, 882.
- [35] X. Bi, J. Li, M. Dahbi, J. Alami, K. Amine, J. Lu, *Adv. Mater.* **2022**, *34*, 2106148.
- [36] S. Nam, M. Mahato, K. Matthews, R. W. Lord, Y. Lee, P. Thangasamy, C. W. Ahn, Y. Gogotsi, I.-K. Oh, *Adv. Funct. Mater.* **2023**, *33*, 2210702.
- [37] Z. Chang, J. Xu, X. Zhang, *Adv. Energy Mater.* **2017**, *7*, 1700875.
- [38] G. Hyun, M. Park, G. Bae, J.-w. Chung, Y. Ham, S. Cho, S. Jung, S. Kim, Y. M. Lee, Y.-M. Kang, S. Jeon, *Adv. Funct. Mater.* **2023**, *33*, 2303059.
- [39] Z. Huang, J. Ren, W. Zhang, M. Xie, Y. Li, D. Sun, Y. Shen, Y. Huang, *Adv. Mater.* **2018**, *30*, 1803270.
- [40] A. Kraysberg, Y. Ein-Eli, *J. Power Sources* **2011**, *196*, 886.
- [41] R. S. Assary, J. Lu, P. Du, X. Luo, X. Zhang, Y. Ren, L. A. Curtiss, K. Amine, *ChemSusChem* **2013**, *6*, 51.
- [42] G. Huang, J. Wang, X. Zhang, *ACS Cent. Sci.* **2020**, *6*, 2136.
- [43] K. Chen, G. Huang, J.-L. Ma, J. Wang, D.-Y. Yang, X.-Y. Yang, Y. Yu, X.-B. Zhang, *Angew. Chem., Int. Ed.* **2020**, *59*, 16661.
- [44] M. C. Policano, C. G. Anchieta, T. C. M. Nepel, R. M. Filho, G. Doubek, *ACS Appl. Energy Mater.* **2022**, *5*, 9228.
- [45] J.-B. Park, S. H. Lee, H.-G. Jung, D. Aurbach, Y.-K. Sun, *Adv. Mater.* **2018**, *30*, 1704162.
- [46] W.-J. Kwak, J. Park, T. T. Nguyen, H. Kim, H. R. Byon, M. Jang, Y.-K. Sun, *J. Mater. Chem. A* **2019**, *7*, 3857.
- [47] J. Zhang, Y. Zhao, B. Sun, Y. Xie, A. Tkacheva, F. Qiu, P. He, H. Zhou, K. Yan, X. Guo, S. Wang, A. M. McDonagh, Z. Peng, J. Lu, G. Wang, *Sci. Adv.* **2022**, *8*, 1899.
- [48] X. Zhang, Q. Zhang, X.-G. Wang, C. Wang, Y.-N. Chen, Z. Xie, Z. Zhou, *Angew. Chem., Int. Ed.* **2018**, *57*, 12814.
- [49] Y. Yu, G. Huang, J.-Z. Wang, K. Li, J.-L. Ma, X.-B. Zhang, *Adv. Mater.* **2020**, *32*, 2004157.
- [50] X. Zhang, Z. Xie, Z. Zhou, *ChemElectroChem* **2019**, *6*, 1969.
- [51] H. Song, H. Deng, C. Li, N. Feng, P. He, H. Zhou, *Small Methods* **2017**, *1*, 1700135.
- [52] L. Qin, D. Zhai, W. Lv, W. Yang, J. Huang, S. Yao, J. Cui, W.-G. Chong, J.-Q. Huang, F. Kang, J.-K. Kim, Q.-H. Yang, *Nano Energy* **2017**, *40*, 258.
- [53] J. L. Ma, F. L. Meng, Y. Yu, D. P. Liu, J. M. Yan, Y. Zhang, X. B. Zhang, Q. Jiang, *Nat. Chem.* **2019**, *11*, 64.
- [54] A. R. Neale, R. Sharpe, S. R. Yeandel, C.-H. Yen, K. V. Luzyanin, P. Goddard, E. A. Petrucco, L. J. Hardwick, *Adv. Funct. Mater.* **2021**, *31*, 2010627.
- [55] X. Wu, Z. Li, C. Song, L. Chen, P. Dai, P. Zhang, Y. Qiao, L. Huang, S.-G. Sun, *ACS Mater. Lett.* **2022**, *4*, 682.
- [56] Q. Xiong, G. Huang, Y. Yu, C. L. Li, J. C. Li, J. M. Yan, X. B. Zhang, *Angew. Chem., Int. Ed.* **2022**, *61*, 202116635.
- [57] B. G. Kim, J.-S. Kim, J. Min, Y.-H. Lee, J. H. Choi, M. C. Jang, S. A. Freunberger, J. W. Choi, *Adv. Funct. Mater.* **2016**, *26*, 1747.
- [58] Y. Wang, D. Li, S. Zhang, Z. Kang, H. Xie, J. Liu, *J. Power Sources* **2020**, *466*, 228336.
- [59] N. Luo, G.-J. Ji, H.-F. Wang, F. Li, Q.-C. Liu, J.-J. Xu, *ACS Nano* **2020**, *14*, 3281.

- [60] M.-G. Jeong, W.-J. Kwak, J. Y. Kim, J. K. Lee, Y.-K. Sun, H.-G. Jung, *Chem. Eng. J.* **2022**, *427*, 130914.
- [61] H.-D. Lim, H. Park, H. Kim, J. Kim, B. Lee, Y. Bae, H. Gwon, K. Kang, *Angew. Chem., Int. Ed.* **2015**, *54*, 9663.
- [62] G. Chen, W. Li, X. Du, C. Wang, X. Qu, X. Gao, S. Dong, G. Cui, L. Chen, *J. Am. Chem. Soc.* **2023**, *145*, 22158.
- [63] J. Shao, H. Ao, L. Qin, J. Elgin, C. E. Moore, Y. Khalifa, S. Zhang, Y. Wu, *Adv. Mater.* **2023**, *35*, 2306809.
- [64] X. Hu, J. Sun, Z. Li, Q. Zhao, C. Chen, J. Chen, *Angew. Chem., Int. Ed.* **2016**, *55*, 6482.
- [65] X. Lin, Q. Sun, J. T. Kim, X. Li, J. Zhang, X. Sun, *Nano Energy* **2023**, *112*, 108466.
- [66] B. Liu, Y. Sun, L. Liu, J. Chen, B. Yang, S. Xu, X. Yan, *Energy Environ. Sci.* **2019**, *12*, 887.
- [67] U. B. Jensen, S. Lörcher, M. Vagin, J. Chevallier, S. Shipovskov, O. Koroleva, F. Besenbacher, E. E. Ferapontova, *Electrochim. Acta* **2012**, *62*, 218.
- [68] M. He, Y. Li, R. Guo, B. M. Gallant, *J. Phys. Chem. Lett.* **2018**, *9*, 4700.
- [69] M. Gao, D. Cai, S. Luo, Y. Yang, Y. Xie, L. Zhu, Z. Yuan, *J. Mater. Chem. A* **2023**, *11*, 16519.
- [70] H. Gao, Y. Li, R. Guo, B. M. Gallant, *Adv. Energy Mater.* **2019**, *9*, 1900393.
- [71] Y. Wang, Y.-C. Lu, *Energy Storage Mater.* **2020**, *28*, 235.
- [72] H. Gao, B. M. Gallant, *Nat. Rev. Chem.* **2020**, *4*, 566.
- [73] X. P. Zhang, Y. Y. Sun, Z. Sun, C. S. Yang, T. Zhang, *Nat. Commun.* **2019**, *10*, 3543.
- [74] G. Cong, W. Wang, N.-C. Lai, Z. Liang, Y.-C. Lu, *Nat. Mater.* **2019**, *18*, 390.
- [75] K. Hu, L. Qin, S. Zhang, J. Zheng, J. Sun, Y. Ito, Y. Wu, *ACS Energy Lett.* **2020**, *5*, 1788.
- [76] X. Chi, M. Li, J. Di, P. Bai, L. Song, X. Wang, F. Li, S. Liang, J. Xu, J. Yu, *Nature* **2021**, *592*, 551.
- [77] Y. He, L. Ding, J. Cheng, S. Mei, X. Xie, Z. Zheng, W. Pan, Y. Qin, F. Huang, Y. Peng, Z. Deng, *Adv. Mater.* **2023**, *35*, 2308134.
- [78] K. Xu, *Chem. Rev.* **2004**, *104*, 4303.
- [79] J. Wang, L. Ma, J. Xu, Y. Xu, K. Sun, Z. Peng, *SusMat* **2021**, *1*, 345.
- [80] R. Black, B. Adams, L. F. Nazar, *Adv. Energy Mater.* **2012**, *2*, 801.
- [81] J. R. Harding, C. V. Amanchukwu, P. T. Hammond, Y. Shao-Horn, *Adv. Energy Mater.* **2015**, *119*, 6947.
- [82] H. Wang, K. Xie, *Electrochim. Acta* **2012**, *64*, 29.
- [83] S. R. Gowda, A. Brunet, G. M. Wallraff, B. D. McCloskey, *J. Phys. Chem. Lett.* **2013**, *4*, 276.
- [84] K. Chen, G. Huang, X.-B. Zhang, *Chin. J. Chem.* **2021**, *39*, 32.
- [85] J.-L. Shui, J. S. Okasinski, P. Kenesei, H. A. Dobbs, D. Zhao, J. D. Almer, D.-J. Liu, *Nat. Commun.* **2013**, *4*, 2255.
- [86] J. Lei, Z. Gao, L. Tang, L. Zhong, J. Li, Y. Zhang, T. Liu, *Adv. Sci.* **2022**, *9*, 2103760.
- [87] H.-K. Lim, H.-D. Lim, K.-Y. Park, D.-H. Seo, H. Gwon, J. Hong, W. A. Goddard III, H. Kim, K. Kang, *J. Am. Chem. Soc.* **2013**, *135*, 9733.
- [88] F. Meng, J. Qin, X. Xiong, X. Li, R. Hu, *Energy Environ. Mater.* **2023**, *6*, e12298.
- [89] Z. Zhang, S. Wu, C. Yang, L. Zheng, D. Xu, R. Zha, L. Tang, K. Cao, X.-g. Wang, Z. Zhou, *Angew. Chem., Int. Ed.* **2019**, *58*, 17782.
- [90] M. Asadi, B. Sayahpour, P. Abbasi, A. T. Ngo, K. Karis, J. R. Jokisaari, C. Liu, B. Narayanan, M. Gerard, P. Yasaei, X. Hu, A. Mukherjee, K. C. Lau, R. S. Assary, F. Khalili-Araghi, R. F. Klie, L. A. Curtiss, A. Salehi-Khojin, *Nature* **2018**, *555*, 502.
- [91] Y. Jiao, J. Qin, H. M. K. Sari, D. Li, X. Li, X. Sun, *Energy Storage Mater.* **2021**, *34*, 148.
- [92] E. R. Ezeigwe, L. Dong, R. Manjunatha, Y. Zuo, S.-Q. Deng, M. Tan, W. Yan, J. Zhang, D. P. Wilkinson, *Nano Energy* **2022**, *95*, 106964.
- [93] H.-W. Lee, H. Kim, H.-G. Jung, Y.-K. Sun, W.-J. Kwak, *Adv. Funct. Mater.* **2021**, *31*, 2102442.
- [94] X. Wu, W. Yu, K. Wen, H. Wang, X. Wang, C.-W. Nan, L. Li, *J. Energy Chem.* **2021**, *60*, 135.
- [95] V. Esfahanian, M. T. Dalakeh, N. Aghamirzaie, *Appl. Energy* **2019**, *250*, 1356.
- [96] W. Xu, J. Wang, F. Ding, X. Chen, E. Nasybulin, Y. Zhang, J.-G. Zhang, *Energy Environ. Sci.* **2014**, *7*, 513.
- [97] F. Sun, R. Gao, D. Zhou, M. Osenberg, K. Dong, N. Kardjilov, A. Hilger, H. Markötter, P. M. Bieker, X. Liu, I. Manke, *ACS Energy Lett.* **2019**, *4*, 306.
- [98] C. O. Laoire, S. Mukerjee, K. M. Abraham, E. J. Plichta, M. A. Hendrickson, *Adv. Energy Mater.* **2010**, *114*, 9178.
- [99] Y. Chen, S. A. Freunberger, Z. Peng, F. Bardé, P. G. Bruce, *J. Am. Chem. Soc.* **2012**, *134*, 7952.
- [100] J. Read, *J. Electrochem. Soc.* **2002**, *149*, A1190.
- [101] B. Zhou, L. Guo, Y. Zhang, J. Wang, L. Ma, W. H. Zhang, Z. Fu, Z. Peng, *Adv. Mater.* **2017**, *29*, 1701568.
- [102] S. Zhang, G. Wang, J. Jin, L. Zhang, Z. Wen, *Energy Storage Mater.* **2020**, *28*, 342.
- [103] H. Wan, Y. Sun, W. Cai, Q. Shi, Y. Zhu, Y. Qian, *Adv. Funct. Mater.* **2021**, *32*, 2106984.
- [104] J. Zhang, B. Sun, Y. Zhao, K. Kretschmer, G. Wang, *Angew. Chem., Int. Ed.* **2017**, *56*, 8505.
- [105] S. Ha, Y. Kim, D. Koo, K.-H. Ha, Y. Park, D.-M. Kim, S. Son, T. Yim, K. T. Lee, *J. Mater. Chem. A* **2017**, *5*, 10609.
- [106] D. Wang, F. Zhang, P. He, H. Zhou, *Angew. Chem., Int. Ed.* **2019**, *58*, 2355.
- [107] Y. Yu, Y.-B. Yin, J.-L. Ma, Z.-W. Chang, T. Sun, Y.-H. Zhu, X.-Y. Yang, T. Liu, X.-B. Zhang, *Energy Storage Mater.* **2019**, *18*, 382.
- [108] W.-L. Bai, Z. Zhang, X. Chen, X. Wei, Q. Zhang, Z.-X. Xu, Y.-S. Liu, B. Chang, K.-X. Wang, J.-S. Chen, *Energy Storage Mater.* **2020**, *31*, 373.
- [109] E. Yoo, H. Zhou, *ACS Appl. Mater. Interfaces* **2020**, *12*, 18490.
- [110] D. Li, C. Zhu, M. Zhang, Y. Wang, Z. Kang, Y. Liu, J. Liu, J. Liu, H. Xie, *Chem. Eng. J.* **2021**, *408*, 127328.
- [111] J. Lai, N. Chen, F. Zhang, B. Li, Y. Shang, L. Zhao, L. Li, F. Wu, R. Chen, *Energy Storage Mater.* **2022**, *49*, 401.
- [112] T. Zhang, H. Zhou, *Nat. Commun.* **2013**, *4*, 1817.
- [113] X. Xin, K. Ito, Y. Kubo, *ACS Appl. Mater. Interfaces* **2017**, *9*, 25976.
- [114] H. Guo, G. Hou, J. Guo, X. Ren, X. Ma, L. Dai, S. Guo, J. Lou, J. Feng, L. Zhang, P. Si, L. Ci, *ACS Appl. Energy Mater.* **2018**, *1*, 5511.
- [115] H.-D. Lim, B. Lee, Y. Zheng, J. Hong, J. Kim, H. Gwon, Y. Ko, M. Lee, K. Cho, K. Kang, *Nat. Energy* **2016**, *1*, 16066.
- [116] W. Walker, V. Giordani, J. Uddin, V. S. Bryantsev, G. V. Chase, D. Addison, *J. Am. Chem. Soc.* **2013**, *135*, 2076.
- [117] M. Roberts, R. Younesi, W. Richardson, J. Liu, T. Gustafsson, J. Zhu, K. Edström, *ECS Electrochem. Lett.* **2014**, *3*, A62.
- [118] J. Liu, T. Wu, S. Zhang, D. Li, Y. Wang, H. Xie, J. Yang, G. Sun, *J. Power Sources* **2019**, *439*, 227095.
- [119] Y. Yu, X.-B. Zhang, *Matter* **2019**, *1*, 881.
- [120] W.-J. Kwak, D. Hirshberg, D. Sharon, M. Afri, A. A. Frimer, H.-G. Jung, D. Aurbach, Y.-K. Sun, *Energy Environ. Sci.* **2016**, *9*, 2334.
- [121] H.-D. Lim, H. Song, J. Kim, H. Gwon, Y. Bae, K.-Y. Park, J. Hong, H. Kim, T. Kim, Y. H. Kim, X. Lepró, R. Ovalle-Robles, R. H. Baughman, K. Kang, *Angew. Chem., Int. Ed.* **2014**, *53*, 3926.
- [122] T. A. Galloway, L. J. Hardwick, *J. Phys. Chem. Lett.* **2016**, *7*, 2119.
- [123] B. Liu, W. Xu, P. Yan, S. T. Kim, M. H. Engelhard, X. Sun, D. Mei, J. Cho, C.-M. Wang, J.-G. Zhang, *Adv. Energy Mater.* **2017**, *7*, 1602605.
- [124] W.-J. Kwak, S.-J. Park, H.-G. Jung, Y.-K. Sun, *Adv. Energy Mater.* **2018**, *8*, 1702258.
- [125] X. Zou, Z. Cheng, Q. Lu, K. Liao, R. Ran, W. Zhou, Z. Shao, *ACS Appl. Mater. Interfaces* **2021**, *13*, 53859.
- [126] K. Pranay Reddy, P. Fischer, M. Marinaro, M. Wohlfahrt-Mehrens, *ChemElectroChem* **2018**, *5*, 2758.
- [127] K. Song, D. A. Agyeman, M. Park, J. Yang, Y.-M. Kang, *Adv. Mater.* **2017**, *29*, 1606572.

- [128] Q. Pang, A. Shyamsunder, B. Narayanan, C. Y. Kwok, L. A. Curtiss, L. F. Nazar, *Nat. Energy* **2018**, *3*, 783.
- [129] C. Zhao, J. Liang, X. Li, N. Holmes, C. Wang, J. Wang, F. Zhao, S. Li, Q. Sun, X. Yang, J. Liang, X. Lin, W. Li, R. Li, S. Zhao, H. Huang, L. Zhang, S. Lu, X. Sun, *Nano Energy* **2020**, *75*, 105036.
- [130] C. V. Amanchukwu, J. R. Harding, Y. Shao-Horn, P. T. Hammond, *Chem. Mater.* **2015**, *27*, 550.
- [131] T. Yang, C. Shu, R. Zheng, M. Li, Z. Hou, P. Hei, Q. Zhang, D. Mei, J. Long, *ACS Sustainable Chem. Eng.* **2019**, *7*, 17362.
- [132] W. Yu, C. Xue, B. Hu, B. Xu, L. Li, C.-W. Nan, *Energy Storage Mater.* **2020**, *27*, 244.
- [133] C. Wang, Z. Guo, S. Zhang, G. Chen, S. Dong, G. Cui, *Energy Storage Mater.* **2021**, *43*, 221.
- [134] X. B. Zhu, T. S. Zhao, Z. H. Wei, P. Tan, L. An, *Energy Environ. Sci.* **2015**, *8*, 3745.
- [135] H. Kitaura, H. Zhou, *Adv. Energy Mater.* **2012**, *2*, 889.
- [136] X. Liu, D. Ren, H. Hsu, X. Feng, G.-L. Xu, M. Zhuang, H. Gao, L. Lu, X. Han, Z. Chu, J. Li, X. He, K. Amine, M. Ouyang, *Joule* **2018**, *2*, 2047.
- [137] A. Wang, X. Zhang, Y.-W. Yang, J. Huang, X. Liu, J. Luo, *Chem* **2018**, *4*, 2192.
- [138] C. Zhao, Q. Sun, J. Luo, J. Liang, Y. Liu, L. Zhang, J. Wang, S. Deng, X. Lin, X. Yang, H. Huang, S. Zhao, L. Zhang, S. Lu, X. Sun, *Chem. Mater.* **2020**, *32*, 10113.
- [139] J. Chen, Y. Wang, S. Li, H. Chen, X. Qiao, J. Zhao, Y. Ma, H. N. Alshareef, *Adv. Sci.* **2023**, *10*, 2205695.
- [140] Z. Guo, C. Li, J. Liu, Y. Wang, Y. Xia, *Angew. Chem., Int. Ed.* **2017**, *56*, 7505.
- [141] B. Liu, J.-G. Zhang, W. Xu, *Joule* **2018**, *2*, 833.
- [142] J. Feng, B. Ge, J. Wang, L. Zhang, D. Liu, G. Zou, J. S. Tse, C. Fernandez, X. Yan, Q. Peng, *J. Power Sources* **2023**, *560*, 232697.
- [143] G. Huang, J. Han, C. Yang, Z. Wang, T. Fujita, A. Hirata, M. Chen, *NPG Asia Mater* **2018**, *10*, 1037.
- [144] H. Guo, G. Hou, D. Li, Q. Sun, Q. Ai, P. Si, G. Min, J. Lou, J. Feng, L. Ci, *ACS Appl. Mater. Interfaces* **2019**, *11*, 30793.
- [145] W.-J. Kwak, H.-J. Shin, J. Reiter, N. Tsiouvaras, J. Hassoun, S. Passerini, B. Scrosati, Y.-K. Sun, *J. Mater. Chem. A* **2016**, *4*, 10467.
- [146] D. Hirshberg, D. Sharon, E. De La Llave, M. Afri, A. A. Frimer, W. J. Kwak, Y. K. Sun, D. Aurbach, *ACS Appl. Mater. Interfaces* **2017**, *9*, 4352.
- [147] Z. Luo, G. Zhu, L. Yin, F. Li, B. B. Xu, L. Dala, X. Liu, K. Luo, *ACS Appl. Mater. Interfaces* **2020**, *12*, 27316.
- [148] Z. Guo, Q. Zhang, C. Wang, Y. Zhang, S. Dong, G. Cui, *Adv. Funct. Mater.* **2021**, *32*, 2108993.
- [149] Q. C. Liu, J. J. Xu, S. Yuan, Z. W. Chang, D. Xu, Y. B. Yin, L. Li, H. X. Zhong, Y. S. Jiang, J. M. Yan, X. B. Zhang, *Adv. Mater.* **2015**, *27*, 5241.
- [150] S. Jung, Z. L. Brown, J. Kim, B. L. Lucht, *Energy Environ. Sci.* **2018**, *11*, 2600.
- [151] Y. Gao, Z. Hou, R. Zhou, D. Wang, X. Guo, Y. Zhu, B. Zhang, *Adv. Funct. Mater.* **2022**, *32*, 2112399.
- [152] B. Li, Y. Chao, M. Li, Y. Xiao, R. Li, K. Yang, X. Cui, G. Xu, L. Li, C. Yang, Y. Yu, D. P. Wilkinson, J. Zhang, *Electrochem. Energy R.* **2023**, *6*, 7.
- [153] M. Zhu, Z. Fan, K. Xu, Y. Fang, W. Sun, Y. Zhu, *Adv. Funct. Mater.* **2022**, *32*, 2112645.
- [154] K. Liao, S. Wu, X. Mu, Q. Lu, M. Han, P. He, Z. Shao, H. Zhou, *Adv. Mater.* **2018**, *30*, 1705711.
- [155] J. Chen, D. Li, K. Lin, X. Ke, Y. Cheng, Z. Shi, *J. Power Sources* **2022**, *540*, 231603.
- [156] Y. Wang, M. Li, F. Yang, J. Mao, Z. Guo, *Energy Mater. Dev.* **2023**, *1*, 9370005.
- [157] T. Osaka, T. Momma, T. Tajima, Y. Matsumoto, *J. Electrochem. Soc.* **1995**, *142*, 1057.
- [158] T. Yang, P. Jia, Q. Liu, L. Zhang, C. Du, J. Chen, H. Ye, X. Li, Y. Li, T. Shen, Y. Tang, J. Huang, *Angew. Chem., Int. Ed.* **2018**, *57*, 12750.
- [159] Z. Wang, Z. Sun, J. Li, Y. Shi, C. Sun, B. An, H.-M. Cheng, F. Li, *Chem. Soc. Rev.* **2021**, *50*, 3178.
- [160] P. Zhang, M. Ding, X. Li, C. Li, Z. Li, L. Yin, *Adv. Energy Mater.* **2020**, *10*, 2001789.
- [161] B. D. McCloskey, D. S. Bethune, R. M. Shelby, T. Mori, R. Scheffler, A. Speidel, M. Sherwood, A. C. Luntz, *J. Phys. Chem. Lett.* **2012**, *3*, 3043.
- [162] L. Ye, M. Liao, H. Sun, Y. Yang, C. Tang, Y. Zhao, L. Wang, Y. Xu, L. Zhang, B. Wang, F. Xu, X. Sun, Y. Zhang, H. Dai, P. G. Bruce, H. Peng, *Angew. Chem., Int. Ed.* **2019**, *58*, 2437.
- [163] F. Guo, T. Kang, Z. Liu, B. Tong, L. Guo, Y. Wang, C. Liu, X. Chen, Y. Zhao, Y. Shen, W. Lu, L. Chen, Z. Peng, *Nano Lett.* **2019**, *19*, 6377.
- [164] G. A. Elia, D. Bresser, J. Reiter, P. Oberhumer, Y.-K. Sun, B. Scrosati, S. Passerini, J. Hassoun, *ACS Appl. Mater. Interfaces* **2015**, *7*, 22638.
- [165] H. Deng, Y. Qiao, S. Wu, F. Qiu, N. Zhang, P. He, H. Zhou, *ACS Appl. Mater. Interfaces* **2019**, *11*, 4908.
- [166] C. Huang, B. Guo, X. Wang, Q. Cao, D. Zhang, J. Huang, J.-Z. Jiang, *Adv. Mater.* **2024**, *36*, 2309732.
- [167] S. Wu, K. Zhu, J. Tang, K. Liao, S. Bai, J. Yi, Y. Yamauchi, M. Ishida, H. Zhou, *Energy Environ. Sci.* **2016**, *9*, 3262.
- [168] H. Deng, Z. Chang, F. Qiu, Y. Qiao, H. Yang, P. He, H. Zhou, *Adv. Energy Mater.* **2020**, *10*, 1903953.
- [169] Y. Sun, K. Chen, C. Zhang, H. Yu, X. Wang, D. Yang, J. Wang, G. Huang, S. Zhang, *Small* **2022**, *18*, 2201470.
- [170] J.-J. Xu, Q.-C. Liu, Y. Yu, J. Wang, J.-M. Yan, X.-B. Zhang, *Adv. Mater.* **2017**, *29*, 1606552.
- [171] Y. Qiao, Y. He, S. Wu, K. Jiang, X. Li, S. Guo, P. He, H. Zhou, *ACS Energy Lett.* **2018**, *3*, 463.
- [172] Y. Ding, Y. Li, M. Wu, H. Zhao, Q. Li, Z.-S. Wu, *Energy Storage Mater.* **2020**, *31*, 470.
- [173] S. H. Lee, J.-B. Park, H.-S. Lim, Y.-K. Sun, *Adv. Energy Mater.* **2017**, *7*, 1602417.
- [174] L. Shi, Z. Li, Y. Li, G. Wang, M. Wu, Z. Wen, *ACS Appl. Mater. Interfaces* **2021**, *13*, 30766.
- [175] E. Peled, D. Golodnitsky, H. Mazor, M. Goor, S. Avshalomov, *J. Power Sources* **2011**, *196*, 6835.
- [176] H. Yadegari, Q. Sun, X. Sun, *Adv. Mater.* **2016**, *28*, 7065.
- [177] L. Qin, N. Xiao, S. Zhang, X. Chen, Y. Wu, *Angew. Chem., Int. Ed.* **2020**, *59*, 10498.
- [178] J. Park, J.-Y. Hwang, W.-J. Kwak, *J. Phys. Chem. Lett.* **2020**, *11*, 7849.
- [179] X. Lin, Y. Sun, Q. Sun, J. Luo, Y. Zhao, C. Zhao, X. Yang, C. Wang, H. Huo, R. Li, X. Sun, *Adv. Energy Mater.* **2021**, *11*, 2003789.
- [180] S. Wu, Y. Qiao, K. Jiang, Y. He, S. Guo, H. Zhou, *Adv. Funct. Mater.* **2018**, *28*, 1706374.
- [181] W. Yu, K. C. Lau, Y. Lei, R. Liu, L. Qin, W. Yang, B. Li, L. A. Curtiss, D. Zhai, F. Kang, *ACS Appl. Mater. Interfaces* **2017**, *9*, 31871.
- [182] X. Bi, R. Wang, Y. Yuan, D. Zhang, T. Zhang, L. Ma, T. Wu, R. Shahbazian-Yassar, K. Amine, J. Lu, *Nano Lett.* **2020**, *20*, 4681.
- [183] P. Yang, J.-M. Tarascon, *Nat. Mater.* **2012**, *11*, 560.
- [184] K. G. Gallagher, S. Goebel, T. Greszler, M. Mathias, W. Oelerich, D. Eroglu, V. Srinivasan, *Energy Environ. Sci.* **2014**, *7*, 1555.
- [185] H. Yang, Y. Qiao, Z. Chang, H. Deng, P. He, H. Zhou, *Adv. Mater.* **2021**, *33*, 2100827.
- [186] L. Chen, J. Yang, Z. Lu, P. Dai, X. Wu, Y. Hong, L. Xiao, L. Huang, H. Bai, S.-G. Sun, *J. Mater. Chem. A* **2022**, *10*, 16570.